

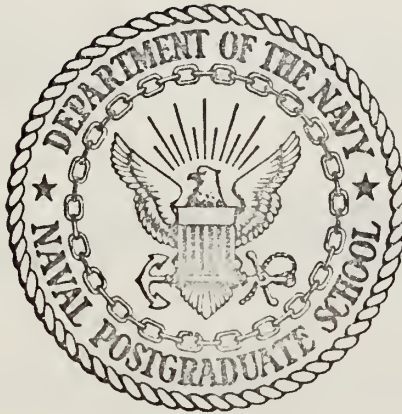
CONSISTENT STRESSES FOR  
THE  
FINITE ELEMENT STIFFNESS METHOD

William Henry Conley



# NAVAL POSTGRADUATE SCHOOL

## Monterey, California



# THESIS

CONSISTENT STRESSES FOR  
THE  
FINITE ELEMENT STIFFNESS METHOD

by

William Henry Conley, Jr.

Thesis Advisor:

D. Salinas

December 1972

T155069

*Approved for public release; distribution unlimited.*



Consistent Stresses for  
the  
Finite Element Stiffness Method

by

William Henry Conley, Jr.  
Lieutenant, United States Navy  
BCE, Marquette University, 1965

Submitted in partial fulfillment  
of the requirements for the degree of

MASTER OF SCIENCE IN MECHANICAL ENGINEERING

from the  
NAVAL POSTGRADUATE SCHOOL  
December 1972



## ABSTRACT

Conjugate basis functions which are continuous throughout a model are used to approximate a stress field. This conjugate approximation has less mean error than approximations calculated using conventional finite element methods and is a better approximation at extreme values of stress. This thesis consists of two major parts. The appropriate analytic expressions for conjugate stress fields are set forth and applied to the constant strain triangle finite element. Analyses are then performed with these new stress calculations and the results compared to some previous stress calculations.





## TABLE OF CONTENTS

I.	INTRODUCTION -----	12
	A. BACKGROUND -----	12
	B. SCOPE AND OBJECTIVES -----	13
II.	CONJUGATE APPROXIMATION THEORY -----	14
	A. MODELING A FUNCTION -----	14
	B. INTERPOLATION FUNCTIONS -----	15
	C. INCIDENCE OPERATORS AND ASSEMBLY -----	17
	D. FUNDAMENTAL MATRIX -----	19
	E. CONJUGATE SPACES -----	20
	F. APPLICATION OF THEORY TO FINITE ELEMENT ---	22
	G. BEST APPROXIMATION -----	23
III.	APPLICATIONS TO DEMONSTRATIVE EXAMPLES -----	26
	A. ONE-DIMENSIONAL PROBLEMS -----	26
	1. Nonlinear Displacement and Linear Properties -----	27
	a. Statement of Problem -----	28
	b. Global Interpolation Functions ----	28
	c. Local Fundamental Matrix -----	30
	d. Global Fundamental Matrix -----	30
	e. Local Conjugate Basis Functions ---	32
	f. Conjugate Nodal Components and Global Representation -----	35
	g. Conventional Finite Element Solution -----	36
	2. Linear Displacement Model and Linear Properties -----	37



3.	Linear Displacement Model and Constant Properties -----	41
4.	Uniform Strain -----	42
5.	Discontinuous Displacement -----	43
a.	Displacement at Node 3 -----	44
b.	Displacement at Node 2 -----	45
B.	TWO-DIMENSIONAL IN-PLANE PROBLEMS -----	46
1.	MODEL A WITH UNIFORM EDGE DIS- PLACEMENT -----	49
2.	MODEL B WITH UNIFORM EDGE DIS- PLACEMENT -----	50
3.	MODEL B WITH UNIFORM EDGE DIS- PLACEMENT, MODIFIED -----	51
4.	MODEL A WITH LINEAR EDGE DIS- PLACEMENT -----	52
5.	MODEL B WITH LINEAR EDGE DIS- PLACEMENT -----	53
6.	MODEL B WITH PIECEWISE LINEAR EDGE DISPLACEMENT -----	55
7.	MODEL A WITH CENTER NODE DIS- PLACEMENT -----	56
8.	MODEL A WITH CENTER NODE DIS- PLACEMENT, MODIFIED -----	57
9.	MODEL B WITH CENTER NODE DIS- PLACEMENT -----	58
10.	MODEL B WITH UNIFORM CENTERLINE DISPLACEMENT -----	59
11.	MODEL B MODIFIED, WITH UNIFORM CENTERLINE DISPLACEMENT -----	60
12.	MODEL B TAPERED WITH UNIFORM EDGE DISPLACEMENT -----	61
13.	COMPOSITE MATERIAL MODELS WITH UNIFORM EDGE DISPLACEMENT -----	62



IV.	THE COMPUTER PROGRAM DEVELOPMENT -----	70
V.	CONCLUSIONS AND RECOMMENDATIONS -----	75
APPENDIX A:	THE IN-PLANE PROBLEM -----	77
APPENDIX B:	THE FINITE ELEMENT METHOD -----	80
APPENDIX C:	COMPUTER PROGRAM -----	85
LIST OF REFERENCES	-----	99
INITIAL DISTRIBUTION LIST	-----	100
FORM DD 1473	-----	101



## LIST OF TABLES

I. Summary of Results for Problems III A1 and III A2 -----	40
II. Comparison of CBM Computer Time in Seconds with LST and PLISOP Time Usage for Similar Problems -----	63





# LIST OF FIGURES

1. Modeling a Bar -----	14
2. Global and Local Functions -----	15
3. Local Interpolation Functions -----	16
4. Approximation to Local Function -----	17
5. A Global Interpolation Function -----	19
6. Best Approximation -----	25
7. One- and Two-Dimensional Domains -----	26
8. Model for Problem III A1 -----	27
9. Set of Global Interpolation Functions -----	29
10. Local Conjugate Basis Functions -----	34
11. Assumed Linear Displacement -----	38
12. Exact Stress Distribution and Approximations to the Exact Stress -----	39
13. $\sigma(x)$ vs $x$ for $k(x) = 1$ -----	42
14. $\sigma(x)$ vs $x$ for Uniform Strain -----	43
15. $\sigma(x)$ vs $x$ for Displacement at Node 3 -----	45
16. $\sigma(x)$ vs $x$ for Displacement at Node 2 -----	46
17. Typical Two-Dimensional Models -----	47
18. Reference System -----	48
19. $\sigma_x$ (PSI x $10^4$ ) for Problem III B1 -----	49
20. $\sigma_x$ (PSI x $10^4$ ) for Problem III B2 -----	50
21. $\sigma_x$ (PSI x $10^4$ ) for Problem III B3 -----	51
22. $\sigma_x$ (PSI x $10^4$ ) for Problem III B4 -----	52
23. $\sigma_x(o)$ vs $y$ for Problem III B4 -----	53
24. $\sigma_x$ (PSI x $10^4$ ) for Problem III B5 -----	54



25.	$\sigma_x$ (PSI x $10^4$ ) for Problem III B6	55
26.	$\sigma_x$ (PSI x $10^4$ ) for Problem III B7	56
27.	$\sigma_x$ (PSI x $10^4$ ) for Problem III B8	57
28.	$\sigma_x$ (PSI x $10^4$ ) for Problem III B9	58
29.	$\sigma_x$ (PSI x $10^4$ ) for Problem III B10	59
30.	$\sigma_x$ (PSI x $10^4$ ) for Problem III B11	60
31.	$\sigma_x$ (PSI x $10^4$ ) for Problem III B12	61
32.	Finite Element Grid System, 124 DOF	64
33.	Finite Element Grid System, 242 DOF	65
34.	Finite Element Grid System for PLISOP, 204 DOF	66
35.	$\sigma_x$ (x,o) (PSI x $10^5$ ) for Problem III B13	67
36.	$\sigma_x$ (x=y) (PSI x $10^5$ ) for Problem III B13	68
37.	$\sigma_x$ (5.2,y) (PSI x $10^5$ ) for Problem III B13	69
A-1.	The In-Plane Problem	77
B-1.	Area Coordinates	81
B-2.	The Linear Strain Triangle	82
B-3.	12 Node PLISOP Element	83



## LIST OF SYMBOLS

$C$	Global Fundamental Matrix (GFM)
$c$	Local Fundamental Matrix
$E$	Total Number of Elements in a Model
$e$	Element Number
$F(x), G(x)$	Functions
$\bar{F}(x)$	Approximation to $F(x)$
$F^\Delta$	Value of $F(x)$ at Node $\Delta$
$F^\Delta$	Value of $F(x)$ at Node $\Delta$ in the Conjugate Basis
$f^e$	Function Defined for Element $e$
$\bar{f}^e$	Approximation to $f^e$
$f_e^N$	Value of $\bar{f}^e$ at Node $N$
$f_N^e$	Value of $\bar{f}^e$ at Node $N$ in Conjugate Basis
$G$	Total Number of Nodes in a Global System
$N, M$	Number of a Node in a Local System
$N_e$	Total Number of Nodes in a Local System
$R$	The Domain of a Function
$\bar{R}$	The Domain of the Approximation
$r_e$	The Domain of an Element
$X$	Location in the Domain $R$
$x$	Location in the Domain $r_e$
$x_e^N$	Node $N$ of Element $e$
$x, y, z$	Coordinate axis
$u, v, w$	Displacements along Coordinate Axis
$\Delta, I$	The Number of a Node in a Global System
$\Lambda$	A Mapping Function



$\Phi$	The Space Spanned by $\phi_{\Delta}$ Bases
$\phi_{\Delta}$	A Global Interpolation Function for Node $\Delta$
$\phi^{\Delta}$	A Conjugate Basis Global Interpolation Function for Node $\Delta$
$\Omega$	A Decomposition Function
$\epsilon$	Strain
$\zeta$	Local Coordinate System with Domain $[0,1]$
$\mu$	Poisson's Ratio
$\sigma$	Stress, PSI
$\psi_N^e$	Local Interpolation Function for Element, e, Node, N.
$\psi_e^N$	Conjugate Basis Local Interpolation Function for Element, e, Node, N.
$\{\phi_{\Delta}\}$	A Set of Global Interpolation Functions
$\langle a, b \rangle$	The Inner Product of a and b
$[c, d]$	The Closed Region Including End Points c and d





## ACKNOWLEDGEMENT

The author is grateful to Professor David Salinas for his aid and guidance throughout this project. Gratitude is also due Professor Gilles Cantin for his assistance in computer programming and in reading the manuscript. Most of all, the author wishes to thank his wife for all she has done and given up to aid in the completion of this work.



## I. INTRODUCTION

### A. BACKGROUND

In a recent paper Oden and Brauchli [Ref. 1] state that one of the difficulties encountered in using the finite element method to approximate the stress field in a model has been that the stresses calculated are at best only averages over each element and, in general, are discontinuous between elements. Continuous stresses can be obtained only if strain degrees of freedom (DOF) are introduced at each node. This is achieved at great computational expense. Some of the schemes which are used to calculate the state of stress at a node are mentioned in Ref. 1 and another method which is based on conjugate approximations is proposed. In Ref. 2 Oden expands on this method explaining the theory of modeling a function in general and using conjugate space functions for modeling in particular.

Briefly the methods of evaluating nodal stresses referred to in Ref. 1 include taking an average of the stresses of each element incident at the node; using a weighted average method developed by Wilson [Ref. 3]; using averages based on equating nodal forces and element stresses in a procedure developed by Turner, Martin and Weikel [Ref. 4]; or using stiffness matrices proposed by Gallagher [Ref. 5] which are developed relating both the stress and displacement fields of each element. Among all methods, the



proposed method, using conjugate bases, has been shown to give the best fit in a least squares sense.

## B. SCOPE AND OBJECTIVES

In this thesis the conjugate approximation theory is set forth in detail and is applied to illustrative examples. The appropriate analytic expressions for conjugate stress fields are derived for the constant strain triangle (CST) finite element and incorporated into a CST computer program.

Numerous examples of in-plane problems are worked comparing both the CST solution and the conjugate basis method (CBM) solutions and the exact solution if it is available.

Finally, some conclusions are reached concerning the type of in-plane problems where the CBM may be used successfully and what the cost in additional computer time may be for this continuous best solution.



## II. CONJUGATE APPROXIMATION THEORY

### A. MODELING A FUNCTION

A function  $F(x)$  over a region or domain  $R$  can be modeled by another function  $\bar{F}(x)$  in the domain  $\bar{R}$  where  $\bar{F} \approx F$  and  $\bar{R} \approx R$ . The region  $\bar{R}$  is subdivided into elements where each element has two or more nodes depending on the degree and type of the approximation function over the element. Within  $\bar{R}$  all elements have the same number of nodes and each node in the global model  $\bar{R}$  is designated  $x^\Delta$ , ( $\Delta = 1, G$ ), where  $G$  is the total number of system nodes. The domain of the element  $e$  is  $r_e$  and each node within this local model is designated  $x_e^N$ , ( $N=1, N_e$ ), where  $N_e$  is the number of nodes in an element.

For example, a one-dimensional axial bar may have the following three element representation (here  $\tilde{R} = R$ ).

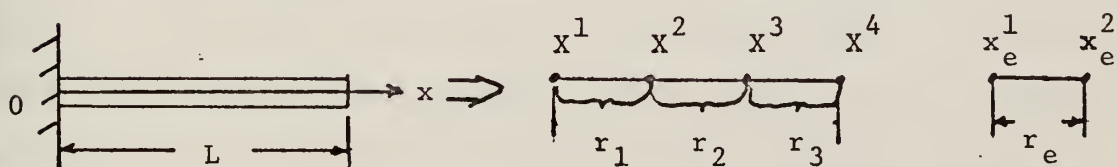


Figure 1. Modeling a Bar.

The value of  $F(x)$  at  $x^\Delta$  is denoted  $F^\Delta$ , that is  $F^\Delta = F(x^\Delta)$ .





Over each element the function  $F(x)$  is represented by a local function,  $f^e(x)$ , which is only defined on the element  $e$ . Its value at  $x_e^N$  is denoted  $f_e^N$ , that is,  $f_e^N = f(x_e^N)$ . Hereafter, the index  $e$  denotes element  $e$ . In the figure below, the functions  $F(x)$ , and  $f_2^N$  for element 2 (i.e.  $e=2$ ) are shown.

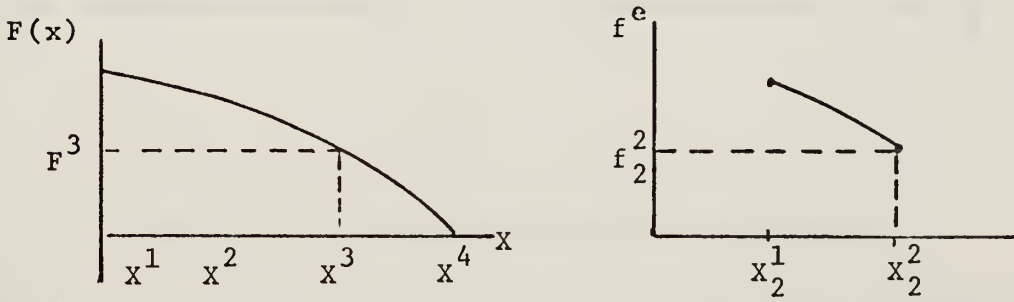


Figure 2. Global and Local Functions.

## B. INTERPOLATION FUNCTIONS

A set of independent local interpolation functions  $\psi_N^e(x)$ , ( $N=1, N_e$ ), is defined over each element such that  $\psi_N^e(x) = 1$  at node  $N$  and zero at all other nodes. (For elements with linear displacement fields, such as the elements used in this thesis,  $\psi_N^e$  is linear between nodes.) For a one-dimensional 2 node element, a set of interpolation functions for representation of a linear field is,

$$\psi_1^e = 1 - \zeta ; \quad \psi_2^e = \zeta \quad (1)$$

where  $\zeta$  is a local coordinate over the closed domain  $[0,1]$  and origin at local node point 1.



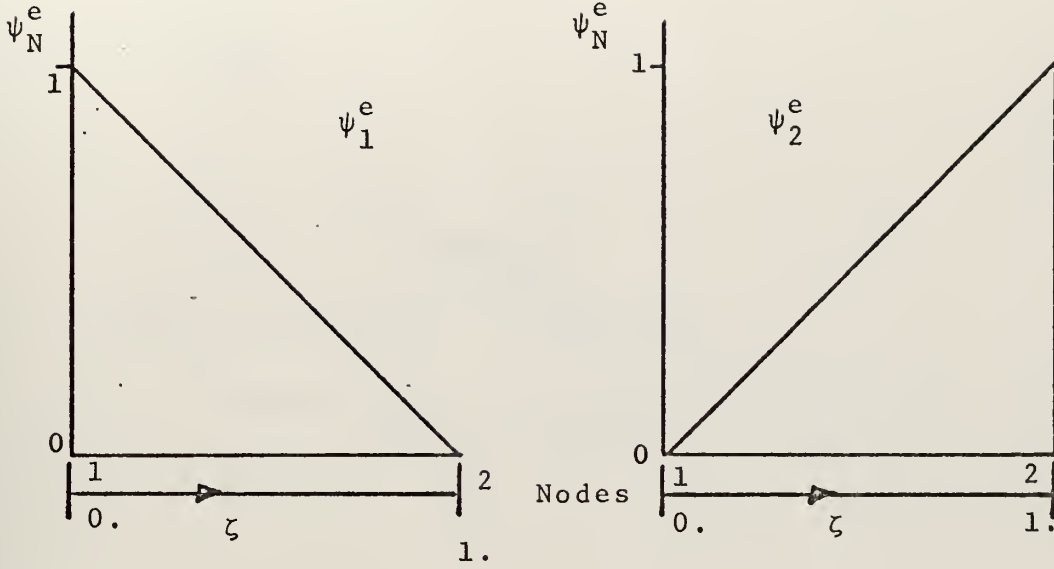


Figure 3. Local Interpolation Functions

The local function,  $f^e(x)$ , is approximated over the element by  $\bar{f}^e(x)$  where

$$\bar{f}^e(x) = f_e^N \psi_N^e(x), \quad N=1, N_e. \quad (2)$$

[The convention  $\bar{f}^e(x) = f_e^N \psi_N^e(x)$  means summation over repeated indices, that is

$$\bar{f}^e(x) = f_e^1 \psi_1^e(x) + f_e^2 \psi_2^e(x) + \dots + f_e^{N_e} \psi_{N_e}^e(x).$$

This summation convention will be used throughout.]

[Note that at a node the value of  $\bar{f}^e(x)$  is  $f_e^N$ .] Here the local function  $f^2(x)$  is modeled by  $\bar{f}^2(x)$  with linear interpolation functions,  $\psi_1^2$  and  $\psi_2^2$ .



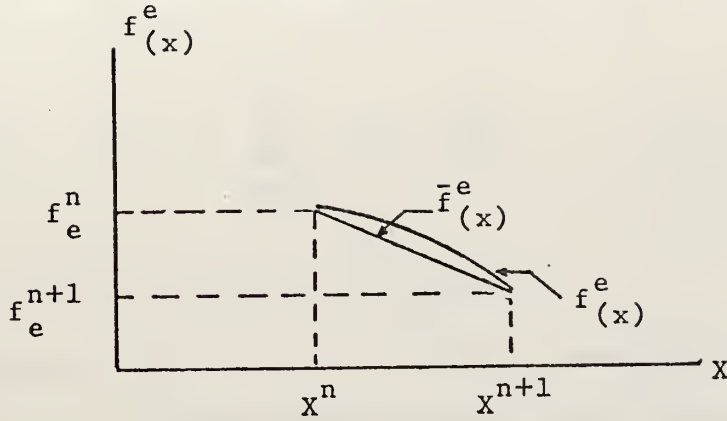


Figure 4. Approximation to Local Function

### C. INCIDENCE OPERATORS AND ASSEMBLY

The function  $\Lambda_N^e$  and  $\Omega_\Delta^e$  are known as incidence operators and are used in relating the global model  $\bar{R}$  to local elements  $r_e$ . They have the value of 1 or 0 as follows:

$$\Lambda_N^e = \begin{cases} 1 & \text{if node } \Delta \text{ in } \bar{R} \text{ is coincident with} \\ & \text{node } N \text{ in } r_e \text{ in the assembled model.} \\ 0 & \text{otherwise} \end{cases} \quad (3a)$$

$$\Omega_\Delta^e = \begin{cases} 1 & \text{if node } N \text{ of element } r_e \text{ is coincident} \\ & \text{with node } \Delta \text{ of the assembled model.} \\ 0 & \text{otherwise} \end{cases} \quad (3b)$$

$\Lambda$  is called a mapping function because it gives the value of a local node to the incident global node. Likewise,  $\Omega$  is called a decomposition function because it gives the global value to the corresponding local node.

$$F^\Delta = \Lambda_N^e f_e^N \quad (\text{Note this is summed over both } e \text{ and } N.) \quad (4)$$

$$f_e^N = \Omega_\Delta^e F^\Delta \quad (5)$$



The model of a function  $F(x)$  in terms of  $\psi_N^e$  element interpolation function can now be given by

$$F(x) \approx \bar{F}(x) = \sum_{e=1}^E \psi_N^e(x) \Omega_{\Delta}^{eN} F^{\Delta} \quad \begin{array}{l} E=1, N_r \\ N=1, N_e \\ \Delta=1, G \end{array} \quad (6)$$

where  $N_r$  is the number of elements.

Equation (6) is true everywhere except at the global nodes with  $m$  elements coincident. Here the value of  $\bar{F}(x)$  is  $m \bar{F}(x)$  times greater than it should be. Accordingly, at the nodes Equation (6) becomes

$$\bar{F}(x) = \frac{1}{m} \sum_{e=1}^E \psi_N^e(x) \Omega_{\Delta}^{eN} F^{\Delta} \quad (7)$$

We note that Equation (7) gives continuity of  $\bar{F}$  at nodal points.

A set of global interpolation functions  $\phi_{\Delta}(x)$  are now defined as follows:

$$\phi_{\Delta}(x) = \begin{array}{ll} \sum_{e=1}^E \psi_N^e(x) \Omega_{\Delta}^{eN} & \text{except at nodes} \\ \frac{1}{m} \sum_{e=1}^E \psi_N^e(x) \Omega_{\Delta}^{eN} & \text{at nodes} \end{array} \quad (8)$$

It will be demonstrated in the examples that  $\phi_{\Delta}(x)$  is a linear combination of the element interpolation functions  $\psi_N^e$ 's. Moreover, since the local  $\psi_N^e$  are independent, the global  $\phi_{\Delta}$  functions are independent also. There is a unique  $\phi_{\Delta}$  for each global node. If the element interpolation functions are independent, the  $\phi_{\Delta}$ 's are independent functions. Now

$$\bar{F}(x) = \phi_{\Delta}(x) F^{\Delta} = \sum_{e=1}^E \psi_N^e(x) f_e^N \quad (9)$$





The domain of a global interpolation function  $\phi_{\Delta}$  extends over all elements incident at  $X^{\Delta}$ . This function has the value 1 at  $X^{\Delta}$  and zero at all other nodal points. For example, with the previous linear interpolation functions, and the three element axial domain, we have

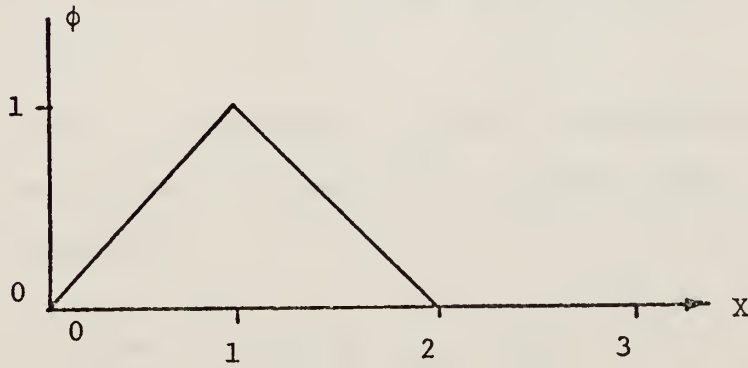


Figure 5. A Global Interpolation Function.

#### D. FUNDAMENTAL MATRIX

The set of  $G$  linearly independent functions  $\{\phi_{\Delta}\}$  form the basis for a  $G$ -dimensional space  $\Phi$  where  $G$  is the total number of global nodes. The fundamental matrix of the space  $\Phi$  is defined as

$$C_{\Delta\Gamma} \equiv \langle \phi_{\Delta}, \phi_{\Gamma} \rangle \quad \Delta, \Gamma = 1, G \quad (10)$$

The notation  $\langle \phi_{\Delta}, \phi_{\Gamma} \rangle$  is used to denote the inner product of  $\phi_{\Delta}$  and  $\phi_{\Gamma}$ . Here the inner product is taken as

$$\langle \phi_{\Delta}, \phi_{\Gamma} \rangle = \int_R \phi_{\Delta} \phi_{\Gamma} dR \quad \Delta, \Gamma = 1, G \quad (11)$$



Since  $\int_R \phi_\Delta \phi_\Delta dR > 0$ ,  $C_{\Delta\Gamma}$  is a positive, definite matrix and its inverse can always be formed. It is defined as

$$(C_{\Delta\Gamma})^{-1} = C^{\Delta\Gamma} \quad (12)$$

This will be the transformation matrix used to form a new set of basis functions in the G-dimensional space. Moreover, since  $\int_R \phi_\Delta \phi_\Gamma dR = \int_R \phi_\Gamma \phi_\Delta dR$ ,  $C_{\Delta\Gamma}$  is also a symmetric matrix.

It is convenient to construct  $C_{\Delta\Gamma}$  from local interpolation functions as follows. Substitute Equation (8) in Equation (10) to obtain

$$C_{\Delta\Gamma} = \langle \phi_\Delta, \phi_\Gamma \rangle = \sum_{e=1}^E \sum_{f=1}^E \Omega_\Delta^e \Omega_\Gamma^f \langle \psi_N^e, \psi_M^f \rangle \quad (13)$$

Here  $\langle \psi_N^e, \psi_M^f \rangle$  is the inner product of the local interpolation functions. It is non zero only if  $e=f$  since each function is only defined on its own element. The inner product  $\langle \psi_N^e, \psi_M^e \rangle$  is called the local fundamental matrix for element  $e$ ,  $c_{NM}^e$ .

Equation (13) now becomes

$$C_{\Delta\Gamma} = \sum_{e=1}^E \Omega_\Delta^e \Omega_\Gamma^e c_{NM}^e \quad (14)$$

## E. CONJUGATE SPACES

A conjugate basis is one which is reciprocally related and interchangeable as to properties with the original basis. A set of G linearly independent functions on  $\bar{R}$ ,



$\{\phi^\Delta\}$ , a so-called conjugate basis set, must satisfy the reciprocity relation,

$$\langle \phi^\Delta, \phi_\Gamma \rangle = \delta_\Gamma^\Delta \quad \text{where } \delta_\Gamma^\Delta = \begin{cases} 1 & \Delta = \Gamma \\ 0 & \Delta \neq \Gamma \end{cases} \quad (15)$$

This means that the sets  $\{\phi_\Delta\}$  and  $\{\phi^\Delta\}$  form a countable biorthogonal basis of the space  $\Phi$ . Any sets  $\{\phi^\Delta\}$  and  $\{\phi_\Delta\}$  which satisfy Equation (15) are referred to as conjugate basis of  $\Phi$ .

In order to define  $\{\phi^\Delta\}$  uniquely, they are formed as follows

$$\phi^\Delta(x) = C^{\Delta\Gamma} \phi_\Gamma(x) \quad (16)$$

It can be shown that the  $\phi^\Delta$ 's are independent functions, and that

$$\phi_\Delta(x) = C_{\Delta\Gamma} \phi^\Gamma(x) \quad (17)$$

Moreover 
$$\begin{aligned} \langle \phi^\Delta, \phi_\Gamma \rangle &= \langle C^{\Delta K} \phi_K, \phi_\Gamma \rangle = C^{\Delta K} \langle \phi_K, \phi_\Gamma \rangle \\ &= C^{\Delta K} C_{K\Gamma} = \delta_\Gamma^\Delta \quad \text{as required by Equation (15).} \end{aligned}$$

Using the incident operators defined in Equation (4), the local conjugate basis interpolation functions are

$$\psi_e^N = \Omega_\Delta^N \phi^\Delta \quad (18)$$

and making the substitutions from Equations (16) and (9) gives

$$\psi_e^N = \Omega_\Delta^N C^{\Delta\Gamma} \phi_\Gamma \quad (19)$$

$$= \Omega_\Delta^N C^{\Delta\Gamma} \sum_{f=1}^E \psi_M^f(x) \Omega_\Gamma^M \quad \begin{matrix} \Delta, \Gamma = 1, G \\ M = 1, N_e \end{matrix} \quad (20)$$

Equation (20) highlights the most important feature of the local conjugate basis functions. The functions for each



node of each element are linear combinations of the basis functions of all G nodes. This gives each local node a basis which is continuous over the entire model. The first example gives a numerical illustration of this.

#### F. APPLICATION OF THEORY TO FINITE ELEMENT

Recall Equation (10) where  $\bar{F}(x) = F^\Delta \phi_\Delta = \sum_{e=1}^E \psi_N^e f_e^N$ . An alternate representation of  $\bar{F}(x)$  in terms of the  $\phi^\Gamma$  basis is obtained as follows

$$\begin{aligned}\bar{F} &= F^\Delta \phi_\Delta = F^\Delta C_{\Delta K} \phi^K \\ &= F_K \phi^K = \sum_{e=1}^E \psi_e^N f_N^e\end{aligned}\quad (21)$$

Here  $F_K$  is the value of  $\bar{F}(x)$  with respect to the conjugate basis. It is calculated by forming the inner product of  $\bar{F}$  and  $\phi_K$ . From Equation (21) we have

$$\begin{aligned}\langle \bar{F}, \phi_K \rangle &= \langle F_N \phi^N, \phi_K \rangle = F_N \langle \phi^N, \phi_K \rangle \\ &= F_N \delta_K^N = F_K\end{aligned}\quad (22)$$

The local values of  $\bar{F}$  are obtained by the usual decomposition,

$$f_N^e = \Omega_N^\Delta F_\Delta = \Omega_N^\Delta \langle \bar{F}, \phi_\Delta \rangle = \langle \bar{F}, \psi_N^e \rangle \quad (23)$$

$$f_e^N = \Omega_N^\Delta F^\Delta = \Omega_N^\Delta \langle \bar{F}, \phi^\Delta \rangle = \langle \bar{F}, \psi_e^N \rangle \quad (24)$$

Now the original function can be approximated in the conjugate basis using Equation (21). This is the procedure used in solving problems using the conjugate basis method (CBM).





## G. BEST APPROXIMATION

Before proceeding, it is important to verify that approximating a function using the conjugate basis functions will give the best approximation in a least square sense.

This is proven simply and clearly with a simple example.

The function  $F(x) = x^2$  is to be approximated in the interval  $x=0$  to  $x=1$  by a linear polynomial  $\tilde{F}(x)$ . Here bases of  $\tilde{F}$  are functions  $\phi_1=1$  and  $\phi_2=x$

$$\tilde{F} = a_1\phi_1 + a_2\phi_2 = a_1(1) + a_2(x) \quad (25)$$

The difference between the actual function and its approximation is called the error,  $E$

$$E = |\tilde{F} - F| \quad (26)$$

The function  $J = J(a_i)$  is a measure of the error over the interval.

$$J(a_i) = \int_0^1 E^2 dx = \int_0^1 [(a_1 + a_2 x) - x^2]^2 dx$$

$$J(a_i) = a_1^2 + a_1 a_2 - \frac{2}{3} a_1 + \frac{1}{3} a_2^2 - \frac{1}{2} a_2 + \frac{1}{5} \quad (27)$$

The error is minimized by setting the partial derivation of  $J(a_i)$ , with respect to  $a_i$ , equal to zero and solving the resulting set of equations for  $a_i$ 's.

$$\frac{\partial J(a_1)}{\partial a_1} = 0 = 2a_1 + a_2 - \frac{2}{3}$$

$$\frac{\partial J(a_2)}{\partial a_2} = 0 = a_1 + \frac{2}{3}a_2 - \frac{1}{2} \quad (28)$$

$$\text{Now } a_1 = -\frac{1}{6}; \quad a_2 = 1 \quad \text{and } \tilde{F} = -\frac{1}{6} + x \quad (29)$$



Using the conjugate basis method with basis functions  $\psi_i$ ,  $\bar{F}$  is determined as follows:

1. Assume the local basis functions are  $\psi_1 = 1 - x$  and  $\psi_2 = x$ .
2. Form the local fundamental matrix  $c_{NM} = \langle \psi_N, \psi_M \rangle$ .

Here we obtain,

$$c_{NM} = \frac{1}{6} \begin{bmatrix} 2 & 1 \\ 1 & 2 \end{bmatrix} \quad (30)$$

3. Take the inverse

$$c^{NM} = \begin{bmatrix} 4 & -2 \\ -2 & 4 \end{bmatrix} \quad (31)$$

4. Form the conjugate basis function  $\psi_e^N = \Omega_{\Delta}^N C^{\Delta\Gamma} \phi_{\Delta}$  in this example  $\phi_{\Gamma} = \psi_{\Gamma}$  because there is just one element.

$$\begin{aligned} \psi^1 &= C^{11} \phi_1 + C^{12} \phi_2 = 4 - 6x \\ \psi^2 &= C^{21} \phi_1 + C^{22} \phi_2 = -2 + 6x \end{aligned} \quad (32)$$

5. Determine  $a_i^e$  where  $a_i^e = \langle F, \psi_i \rangle$

$$a_1 = \int_0^1 x^2 \phi_1 dx = \frac{1}{12}; \quad a_2 = \int_0^1 x^2 \phi_2 dx = \frac{1}{4}$$

6. Approximate  $F(x)$  with  $\bar{F} = \sum_{e=1}^1 a_i^e \psi_e^i \quad i=1,2$

$$\begin{aligned} F &= \frac{1}{12}(4-6x) + \frac{1}{4}(-2+6x) \\ &= -\frac{1}{6} + x \end{aligned} \quad (33)$$



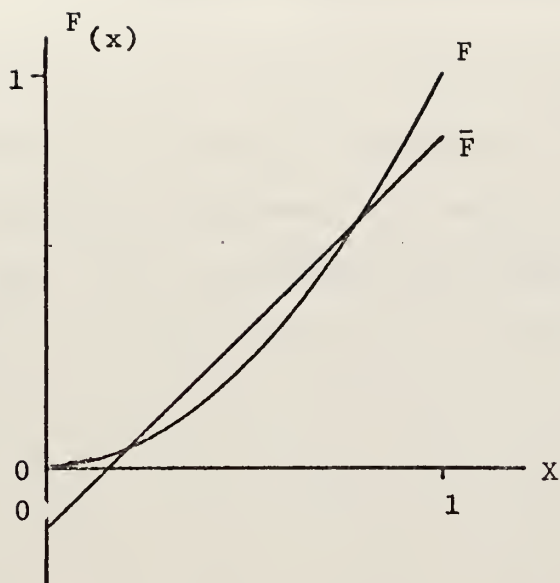


Figure 6. Best Approximation

This is the same approximate function obtained using the previous calculus method. Therefore, the best approximation of a given function  $F(x)$  in the subspace  $\phi$  is the function  $\bar{F}(x)$  whose components are the inner product of  $F(x)$  and the conjugate basis functions. Reference 2 contains a formal proof that the CBM is the best fit in the least square sense.



### III. APPLICATIONS TO DEMONSTRATIVE EXAMPLES

In all of the problems considered in this thesis, the displacement must be in the domain of the structure. For one-dimensional problems, the model is a bar displaced along the  $x$  axis. The two-dimensional model is a plane with displacements in either the  $x$  or  $y$  direction or both.

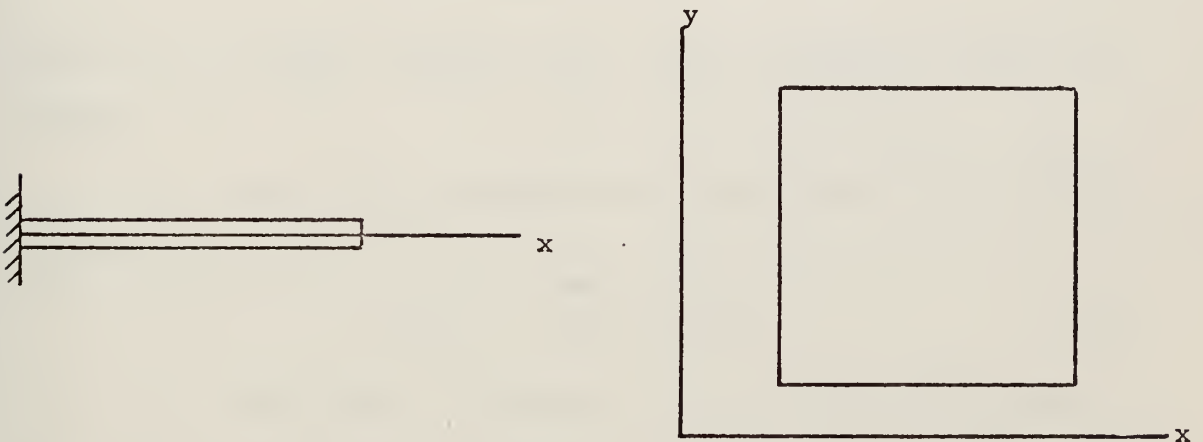


Figure 7. One- and Two-Dimensional Domains.

Appendix A contains a brief summary of the stress-strain and strain-displacement relations for the in-plane problem.

#### A. ONE-DIMENSIONAL PROBLEMS

##### 1. Nonlinear Displacement and Linear Properties

To demonstrate certain properties of conjugate approximation functions, example 9.2 in Ref. 2 will be





explored in detail.

a. Statement of Problem

Determine the stress in a nonhomogeneous, 3 unit length bar based on approximate displacement fields. The stress is given by

$$\sigma(x) = k(x) \frac{du(x)}{dx} \quad (34)$$

where  $k(x) = k_0(1+x)$  (35)

is the material modulus in units of force/length<sup>2</sup> and  $u(x)$  is the displacement field. Assume that

$$u(x) = \alpha \left[ 1 - \frac{x^2}{9} \right] \quad (36)$$

where  $\alpha$  is a small constant and  $x$  is measured in units of length.

With this displacement field, the exact stress distribution is

$$\sigma(x) = - \frac{2\alpha k_0}{9} x(1+x) \quad (37)$$

The model  $\bar{R}$  consists of three one-dimensional elements, each of unit length, that is  $R = \bar{R} = [0, 3] = \bigcup_{e=1}^3 \Omega_e$ .

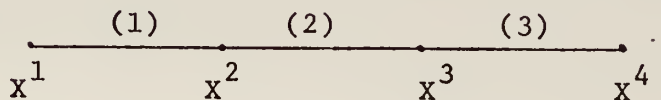


Figure 8. Model for Problem III A1.



The local basis functions, for a linear field, corresponding to a typical element, e, are the interpolation functions shown with Equation (1),

$$\psi_1^e(\xi) = 1 - \xi \quad \text{and} \quad \psi_2^e(\xi) = \xi$$

b. Global Interpolation Functions

The global interpolation functions are calculated using Equation (9),

$$\phi_\Delta(x) = \sum_{e=1}^3 \Omega_\Delta^e \psi_N^e(x) \quad \begin{array}{l} \Delta = 1,4 \\ N = 1,2 \end{array}$$

NOTE: The notation (x) will be omitted unless it is needed for clarity.

The above expression gives,

$$\begin{aligned} \phi_1 &= \Omega_1^1 \psi_1^1 + \Omega_1^2 \psi_1^2 + \Omega_1^3 \psi_1^3 + \Omega_1^4 \psi_1^4 + \Omega_1^5 \psi_1^5 + \Omega_1^6 \psi_1^6 \\ &= 1 \psi_1^1 + 0 + 0 + 0 + 0 + 0 \\ \phi_2 &= \Omega_2^1 \psi_1^1 + \Omega_2^2 \psi_1^2 + \Omega_2^3 \psi_1^3 + \Omega_2^4 \psi_1^4 + \Omega_2^5 \psi_1^5 + \Omega_2^6 \psi_1^6 \\ &= 0 + 1 \psi_1^2 + 1 \psi_1^3 + 0 + 0 + 0 \\ \phi_3 &= \Omega_3^1 \psi_1^1 + \Omega_3^2 \psi_1^2 + \Omega_3^3 \psi_1^3 + \Omega_3^4 \psi_1^4 + \Omega_3^5 \psi_1^5 + \Omega_3^6 \psi_1^6 \\ &= 0 + 0 + 0 + 1 \psi_1^4 + 1 \psi_1^5 + 0 \\ \phi_4 &= \Omega_4^1 \psi_1^1 + \Omega_4^2 \psi_1^2 + \Omega_4^3 \psi_1^3 + \Omega_4^4 \psi_1^4 + \Omega_4^5 \psi_1^5 + \Omega_4^6 \psi_1^6 \\ &= 0 + 0 + 0 + 0 + 0 + 1 \psi_1^6 \end{aligned} \quad (38)$$

These are shown in Figure 9.



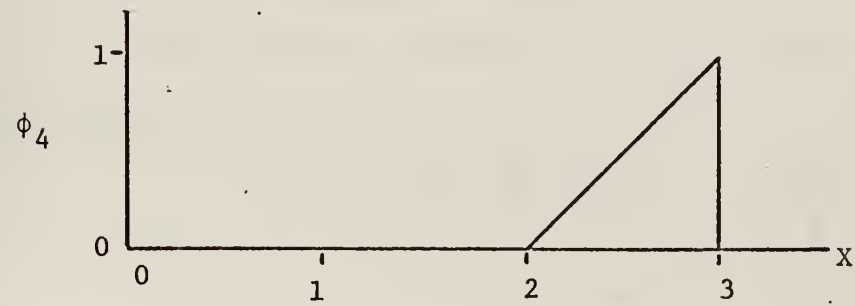
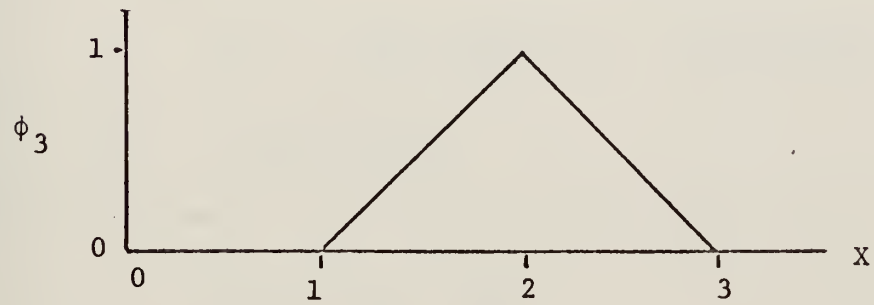
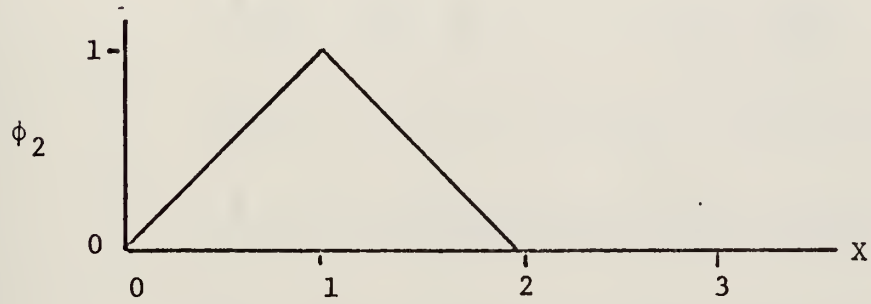
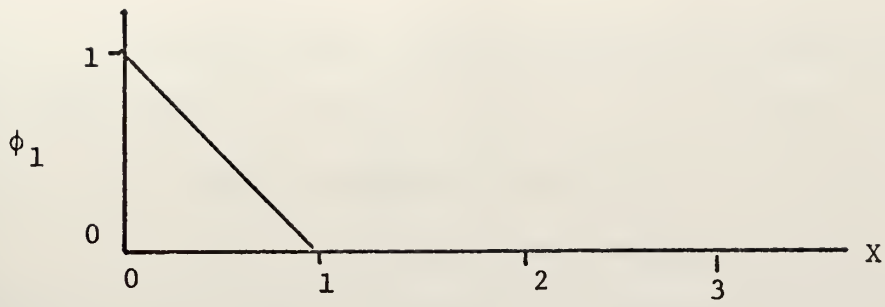


Figure 9. Set of Global Interpolation Functions.



Recall that using Equation (8) the value of  $\phi_{\Delta}$  at a node where 2 or more elements are incident is still 1.

#### c. Local Fundamental Matrix

The local fundamental matrix (LFM) is formed using the local basis functions as discussed in Section II-D.

$$\begin{aligned}
 c_{NM}^e &= \langle \psi_N^e, \psi_M^e \rangle & N, M &= 1, 2 \\
 & & e &= 1, 3 \\
 c_{11}^1 &= \int_0^1 \psi_1^1(\xi) \psi_1^1(\xi) d\xi = \int_0^1 (1-\xi)(1-\xi) d\xi = \frac{1}{3} \\
 c_{12}^1 &= \int_0^1 \psi_1^1(\xi) \psi_2^1(\xi) d\xi = \int_0^1 (1-\xi)\xi d\xi = \frac{1}{6} \\
 c_{21}^1 &= \int_0^1 \psi_2^1(\xi) \psi_1^1(\xi) d\xi = \int_0^1 \xi(1-\xi) d\xi = \frac{1}{6} \\
 c_{22}^1 &= \int_0^1 \psi_2^1(\xi) \psi_2^1(\xi) d\xi = \int_0^1 \xi(\xi) d\xi = \frac{1}{3} \quad (39)
 \end{aligned}$$

$$\text{Now } c_{NM}^1 = \frac{1}{6} \begin{bmatrix} 2 & 1 \\ 1 & 2 \end{bmatrix} \quad (40)$$

Since the elements are geometrically identical, we have

$$c_{NM}^1 = c_{NM}^2 = c_{NM}^3.$$

#### d. Global Fundamental Matrix

The global fundamental matrix (GFM) is formed using Equation (14),

$$C_{\Delta\Gamma} = \sum_{e=1}^E \Omega_{\Delta}^N \Omega_{\Gamma}^M c_{NM}^e \quad \begin{aligned} N, M &= 1, 2 \\ \Delta, \Gamma &= 1, 4 \\ E &= 3 \end{aligned}$$

Since  $C_{\Delta\Gamma}$  is a 4 x 4 symmetric matrix, a total of ten separate calculations would be needed to determine





all of the elements of the GFM. The calculations for  $c_{11}$  and  $c_{22}$  are shown below.

$$\begin{aligned}
 C_{11} &= \frac{1}{\Omega_1 \Omega_1} \frac{1}{\Omega_1} \frac{1}{\Omega_1} \frac{1}{\Omega_1} c_{11} + \frac{1}{\Omega_1 \Omega_1} \frac{1}{\Omega_1} \frac{1}{\Omega_1} \frac{1}{\Omega_1} c_{12} + \frac{1}{\Omega_1 \Omega_1} \frac{1}{\Omega_1} \frac{1}{\Omega_1} \frac{1}{\Omega_1} c_{21} + \frac{1}{\Omega_1 \Omega_1} \frac{1}{\Omega_1} \frac{1}{\Omega_1} \frac{1}{\Omega_1} c_{22} \\
 &+ \frac{2}{\Omega_1 \Omega_1} \frac{2}{\Omega_1} \frac{2}{\Omega_1} \frac{2}{\Omega_1} c_{11} + \frac{2}{\Omega_1 \Omega_1} \frac{2}{\Omega_1} \frac{2}{\Omega_1} \frac{2}{\Omega_1} c_{12} + \frac{2}{\Omega_1 \Omega_1} \frac{2}{\Omega_1} \frac{2}{\Omega_1} \frac{2}{\Omega_1} c_{21} + \frac{2}{\Omega_1 \Omega_1} \frac{2}{\Omega_1} \frac{2}{\Omega_1} \frac{2}{\Omega_1} c_{22} \\
 &+ \frac{3}{\Omega_1 \Omega_1} \frac{3}{\Omega_1} \frac{3}{\Omega_1} \frac{3}{\Omega_1} c_{11} + \frac{3}{\Omega_1 \Omega_1} \frac{3}{\Omega_1} \frac{3}{\Omega_1} \frac{3}{\Omega_1} c_{12} + \frac{3}{\Omega_1 \Omega_1} \frac{3}{\Omega_1} \frac{3}{\Omega_1} \frac{3}{\Omega_1} c_{21} + \frac{3}{\Omega_1 \Omega_1} \frac{3}{\Omega_1} \frac{3}{\Omega_1} \frac{3}{\Omega_1} c_{22} \\
 &= \frac{1}{6} [1 \cdot 1 \cdot 2 + 0 + 0 + 0 + 0 + 0 + 0 + 0 + 0 + 0 + 0 + 0] \\
 &= \frac{2}{6} \\
 C_{22} &= \frac{1}{\Omega_2 \Omega_2} \frac{1}{\Omega_2} \frac{1}{\Omega_2} \frac{1}{\Omega_2} c_{11} + \frac{1}{\Omega_2 \Omega_2} \frac{1}{\Omega_2} \frac{1}{\Omega_2} \frac{1}{\Omega_2} c_{12} + \frac{1}{\Omega_2 \Omega_2} \frac{1}{\Omega_2} \frac{1}{\Omega_2} \frac{1}{\Omega_2} c_{21} + \frac{1}{\Omega_2 \Omega_2} \frac{1}{\Omega_2} \frac{1}{\Omega_2} \frac{1}{\Omega_2} c_{22} \\
 &+ \frac{2}{\Omega_2 \Omega_2} \frac{2}{\Omega_2} \frac{2}{\Omega_2} \frac{2}{\Omega_2} c_{11} + \frac{2}{\Omega_2 \Omega_2} \frac{2}{\Omega_2} \frac{2}{\Omega_2} \frac{2}{\Omega_2} c_{12} + \frac{2}{\Omega_2 \Omega_2} \frac{2}{\Omega_2} \frac{2}{\Omega_2} \frac{2}{\Omega_2} c_{21} + \frac{2}{\Omega_2 \Omega_2} \frac{2}{\Omega_2} \frac{2}{\Omega_2} \frac{2}{\Omega_2} c_{22} \\
 &+ \frac{3}{\Omega_2 \Omega_2} \frac{3}{\Omega_2} \frac{3}{\Omega_2} \frac{3}{\Omega_2} c_{11} + \frac{3}{\Omega_2 \Omega_2} \frac{3}{\Omega_2} \frac{3}{\Omega_2} \frac{3}{\Omega_2} c_{12} + \frac{3}{\Omega_2 \Omega_2} \frac{3}{\Omega_2} \frac{3}{\Omega_2} \frac{3}{\Omega_2} c_{21} + \frac{3}{\Omega_2 \Omega_2} \frac{3}{\Omega_2} \frac{3}{\Omega_2} \frac{3}{\Omega_2} c_{22} \\
 &= \frac{1}{6} [0 + 0 + 0 + 2 + 2 + 0 + 0 + 0 + 0 + 0 + 0 + 0] \\
 &= \frac{4}{6} \tag{41}
 \end{aligned}$$

The complete GFM and its inverse are shown

below.

$$C_{\Delta\Gamma} = \frac{1}{6} \begin{bmatrix} 2 & 1 & 0 & 0 \\ 1 & 4 & 1 & 0 \\ 0 & 1 & 4 & 1 \\ 0 & 0 & 1 & 2 \end{bmatrix} \quad C^{\Delta\Gamma} = \frac{6}{45} \begin{bmatrix} 26 & -7 & 2 & -1 \\ -7 & 14 & -4 & 2 \\ 2 & -4 & 14 & -7 \\ -1 & 2 & -7 & 26 \end{bmatrix} \tag{42}$$

In practice, the entire set of calculations using incidence operators is avoided and the LFM elements are placed in the GFM according to the following scheme.

Each column and each row of the GFM is associated with one and only one global node. Likewise, each column and each row of the LFM is associated with just one



global node. In assembling the GFM, the  $ij$  element from the LFM associated with local nodes  $i,j$  is added to the  $k,l$  GFM element, where global nodes  $k,l$  correspond to local nodes  $i,j$ . If several elements are incident at a global node, then the appropriate elements from each of the connecting elements' LFM will be summed in the GFM. This procedure avoids numerous calculations where the incident operator is zero.

#### e. Local Conjugate Basis Functions

The local conjugate basis functions are calculated using Equation (19),

$$\psi_e^N(x) = \Omega_{\Delta}^N C^{\Delta\Gamma} \phi_{\Gamma}(x) \quad \begin{array}{l} e = 1,3 \\ N = 1,2 \\ \Delta, \Gamma = 1,4 \end{array}$$

The calculation for node 1 of element 1 is shown below.

$$\begin{aligned} \psi_1^1 = & \Omega_1^1 c^{11} \phi_1 + \Omega_1^1 c^{12} \phi_2 + \Omega_1^1 c^{13} \phi_3 + \Omega_1^1 c^{14} \phi_4 \\ & + \Omega_2^1 c^{21} \phi_1 + \Omega_2^1 c^{22} \phi_2 + \Omega_2^1 c^{23} \phi_3 + \Omega_2^1 c^{24} \phi_4 \\ & + \Omega_3^1 c^{31} \phi_1 + \Omega_3^1 c^{32} \phi_2 + \Omega_3^1 c^{33} \phi_3 + \Omega_3^1 c^{34} \phi_4 \\ & + \Omega_4^1 c^{41} \phi_1 + \Omega_4^1 c^{42} \phi_2 + \Omega_4^1 c^{43} \phi_3 + \Omega_4^1 c^{44} \phi_4 \end{aligned} \quad (43)$$

$$\text{For node 1 of element 1 } \Omega_{\Delta}^N = \begin{array}{l} 1 \text{ for } \Omega_1^1 \\ 0 \text{ for all other} \end{array}$$

Therefore, substituting for  $C^{\Delta\Gamma}$  and  $\phi_{\Delta}$  above  $\psi_1^1$  becomes

$$\psi_1^1 = \frac{6}{45} [26 \psi_1^1 - 7(\psi_2^1 + \psi_1^2) + 2(\psi_2^2 + \psi_1^3) - \psi_2^3] \quad (44)$$

where the  $\psi$ 's in brackets are the local basis functions defined in Equation (1).



Notice that only one row of the above calculation was nonzero - that is the row where  $\Omega_{\Delta}^N = 1$ . Using this fact reduces the actual calculations in a manner similar to the method used in forming the GFM.

Consider the nonzero row of the above calculation. Factoring out the common incidence operator leaves four terms which are the products of the  $\Gamma$ th element of the  $\Delta$  row of the GFM inverse times  $\phi_{\Gamma}$ . Recall that at a node  $\phi_{\Gamma} = 1$  and the local conjugate basis functions  $X = X^{\Delta}$  become equal to the  $\Delta$  row of the GFM inverse. This greatly simplifies computer programming of the conjugate basis method.

Returning to the example at hand. Global node 2 is node 2 of element 1 and node 1 of element 2. Therefore,  $\Omega_2^1 = \Omega_2^2 = 1$  and  $\Omega_{\Delta}^2 = \Omega_{\Delta}^1 = 0$  for  $\Delta = 1, 3, \text{ or } 4$ .

Showing only the nonzero terms of the calculation,

$$\begin{aligned}\psi_1^2 &= \psi_2^1 = c^{21}\phi_1 + c^{22}\phi_2 + c^{23}\phi_3 + c^{24}\phi_4 \\ &= \frac{6}{45}[-7\psi_1^1 + 14(\psi_2^1 + \psi_1^2) - 4(\psi_2^2 + \psi_1^3) + 2\psi_2^3] \quad (45)\end{aligned}$$

A similar argument for global nodes 3 and 4 gives

$$\psi_2^2 = \psi_3^1 = \frac{6}{45}[2\psi_1^1 - 4(\psi_2^1 + \psi_1^2) + 14(\psi_2^2 + \psi_1^3) - 7\psi_2^3] \quad (46)$$

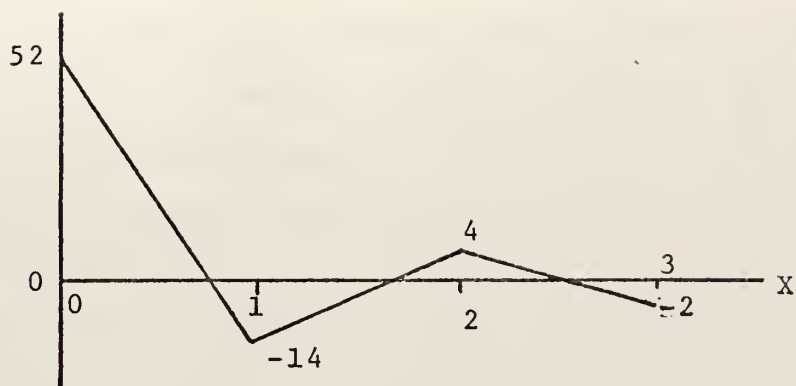
and

$$\psi_3^2 = \frac{6}{45}[-1\psi_1^1 + 2(\psi_2^1 + \psi_1^2) - 7(\psi_2^2 + \psi_1^3) + 26\psi_2^3] \quad (47)$$

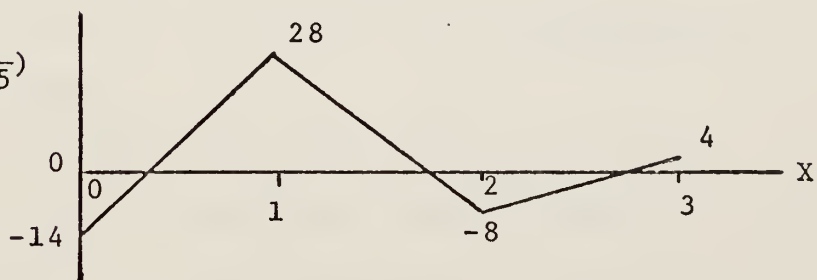
The local conjugate basis functions are shown graphically in Figure 10. Notice that each function is



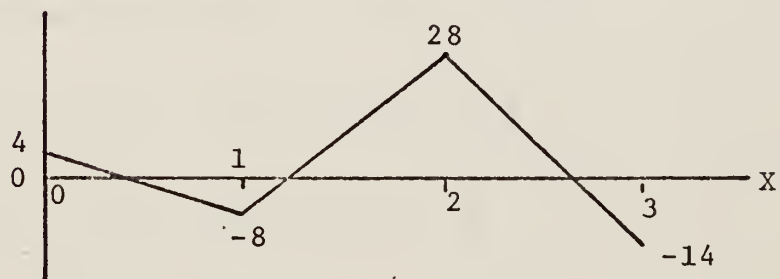
$$\psi_1^1(x) \left(\frac{1}{15}\right)$$



$$\psi_1^2(x) = \psi_2^1(x) \left(\frac{1}{15}\right)$$



$$\psi_2^2(x) = \psi_3^1(x) \left(\frac{1}{15}\right)$$



$$\psi_3^2(x) \left(\frac{1}{15}\right)$$

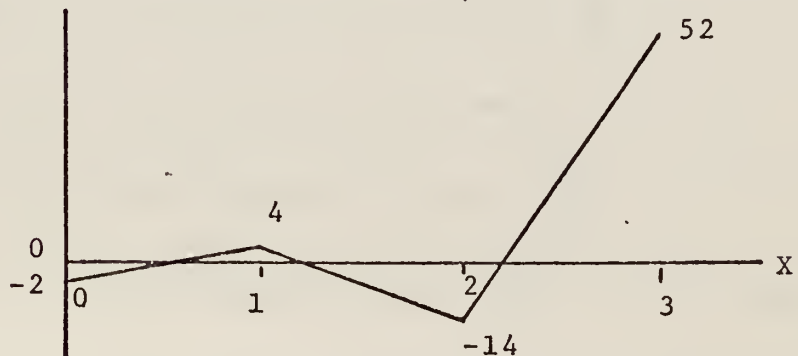


Figure 10. Local Conjugate Basis Functions.





continuous over the domain,  $x$ , and that the effects of nodes remote from the local node being considered diminish as the distance from that node increases.

f. Conjugate Nodal Components and Global Representation

Calculate the conjugate nodal components of the element stress field according to Equation (23).

$$\sigma_N^e = \langle \bar{\sigma}(x), \psi_N^e(x) \rangle$$

Since  $\psi_N^e$  are in terms of  $\xi$ ,  $\sigma(x)$  will be transformed to functions of  $\xi$  also,

$$\begin{aligned}\sigma(\xi) &= 2\xi + 2\xi^2 \quad \text{for } 0 \leq x \leq 1 \\ &= 2\xi^2 + 6\xi + 4 \quad \text{for } 1 \leq x \leq 2 \\ &= 2\xi^2 + 10\xi + 12 \quad \text{for } 2 \leq x \leq 3\end{aligned}$$

a factor of  $-\frac{\alpha k_o}{9}$  has been factored out to enable comparison with the results published in Ref. 2. Now

$$\begin{aligned}\sigma_1^1 &= \int_0^1 (2\xi + 2\xi^2)(1-\xi) d\xi = \frac{3}{6} \\ \sigma_2^1 &= \int_0^1 (2\xi + 2\xi^2)(\xi) d\xi = \frac{7}{6} \\ \sigma_1^2 &= \int_0^1 (2\xi^2 + 6\xi + 4)(1-\xi) d\xi = \frac{19}{6} \\ \sigma_2^2 &= \int_0^1 (2\xi^2 + 6\xi + 4)(\xi) d\xi = \frac{27}{6} \\ \sigma_1^3 &= \int_0^1 (2\xi^2 + 10\xi + 12)(1-\xi) d\xi = \frac{47}{6} \\ \sigma_2^3 &= \int_0^1 (2\xi^2 + 10\xi + 12)(\xi) d\xi = \frac{59}{6}\end{aligned} \quad (48)$$

Now the global stress field can be modeled using Equation

$$(21), \quad \sigma(x) = \sum_{e=1}^3 \sigma_N^e \psi_e^N(x) \quad N = 1, 2$$



At the global nodes we have

$$\begin{aligned}
 \sigma(0.) &= \frac{3}{6} \frac{52}{15} - \frac{7}{6} \frac{14}{15} - \frac{19}{6} \frac{14}{15} + \frac{27}{6} \frac{4}{15} + \frac{47}{6} \frac{4}{15} - \frac{59}{6} \frac{2}{15} \\
 &= -0.33 \\
 \sigma(1.) &= \frac{3}{6} \frac{(-14)}{15} + \frac{28}{15} \left( \frac{7}{6} + \frac{19}{6} \right) - \frac{8}{15} \left( \frac{27}{6} + \frac{47}{6} \right) + \frac{4}{15} \left( \frac{59}{6} \right) \\
 &= 3.43 \tag{49}
 \end{aligned}$$

Similar calculations are made for  $x=2$  and  $x=3$ .

The results are

$$\sigma(2.) = 11.7$$

$$\sigma(3.) = 23.6$$

These results are plotted on Figure 12 and are also shown in Table 1. Since the exact stress field was known, a comparison of accuracy is made.

#### g. Conventional Finite Element Solution (C.F.E.)

Here we suppose the continuous displacement field  $U(x)$  is approximated by the piecewise linear field,  $\bar{U}(x)$  where

$$\bar{U}(x) = \frac{\alpha}{9} [9\phi_1(x) + 8\phi_2(x) + 5\phi_3(x)]. \tag{50}$$

The  $\phi$ 's are shown in Figure 9. This linear field was constructed to give  $\bar{U}(x) = U(x)$  at the nodal points by evaluating  $U(x)$  at the nodes. The strain is now

$$\frac{d\bar{U}(x)}{dx} = -\frac{\alpha}{9} \begin{cases} 9 \frac{d\phi_1}{dx} + 8 \frac{d\phi_2}{dx} = 1 & 0 \leq x \leq 1 \\ 8 \frac{d\phi_2}{dx} + 5 \frac{d\phi_3}{dx} = 3 & 1 \leq x \leq 2 \\ 5 \frac{d\phi_3}{dx} = 5 & 2 \leq x \leq 3 \end{cases} \tag{51}$$



The conventional solution is obtained from

$$\sigma(x) = k(x) \frac{d\bar{U}(x)}{dx} \text{ where the value of } \frac{dU(x)}{dx} \text{ is}$$

given above.

## 2. Linear Displacement Model and Linear Properties

In the first example the exact stress function was known and was used to calculate  $\sigma_N^e(x)$ . Consider the results if the stress field is approximated by

$$\sigma(x) = k(x) \frac{d\bar{U}(x)}{dx} \quad (52)$$

where  $\frac{d\bar{U}(x)}{dx}$  is a constant over each element.

This is the constant strain approximation. Since a constant strain triangle (CST) finite element computer program is used to provide the  $\sigma_N^e$ 's in the two-dimensional problems considered later, using  $\frac{dU}{dx} = \text{constant}$  provides a guide to the error which may be expected.

$U(x)$  as given in Equation (36) is calculated at each node and plotted vs  $x$  below assuming linear displacement between nodes. The slope of each line segment is  $\frac{d\bar{U}}{dx}$  and is shown in parentheses.



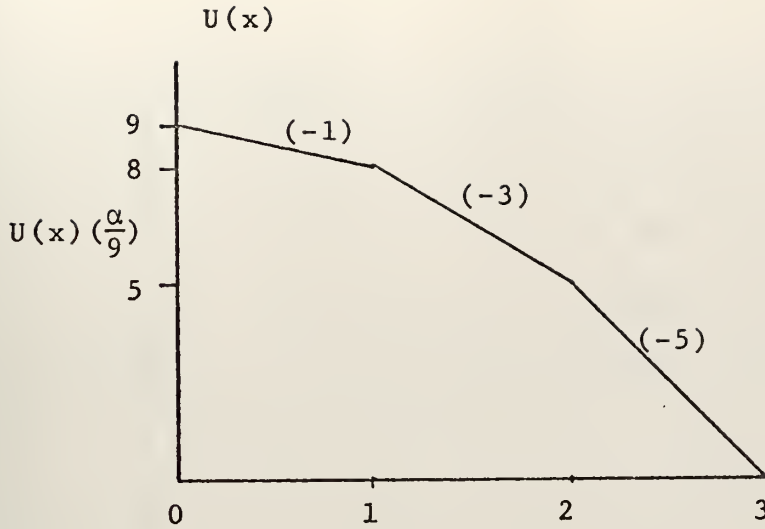


Figure 11. Assumed Linear Displacement Model

The conjugate nodal components,  $\sigma_N^e(x)$ , are now given by

$$\sigma_N^e(x) = - \frac{\alpha k_o}{9} \int_0^L [(1+x) \frac{dU}{dx}] \psi_N^e(x) dx \quad (53)$$

The results of the integration, disregarding the  $-\frac{\alpha k_o}{9}$  factor, are

$$\begin{aligned} \sigma_1^1 &= \frac{4}{6} & \sigma_1^2 &= \frac{21}{6} & \sigma_1^3 &= \frac{50}{6} \\ \sigma_2^1 &= \frac{8}{6} & \sigma_2^2 &= \frac{24}{6} & \sigma_2^3 &= \frac{55}{6} \end{aligned} \quad (54)$$

The conjugate function representation of stress is given by Equation (21) and the results are plotted on Figure 12 and included in Table 1.





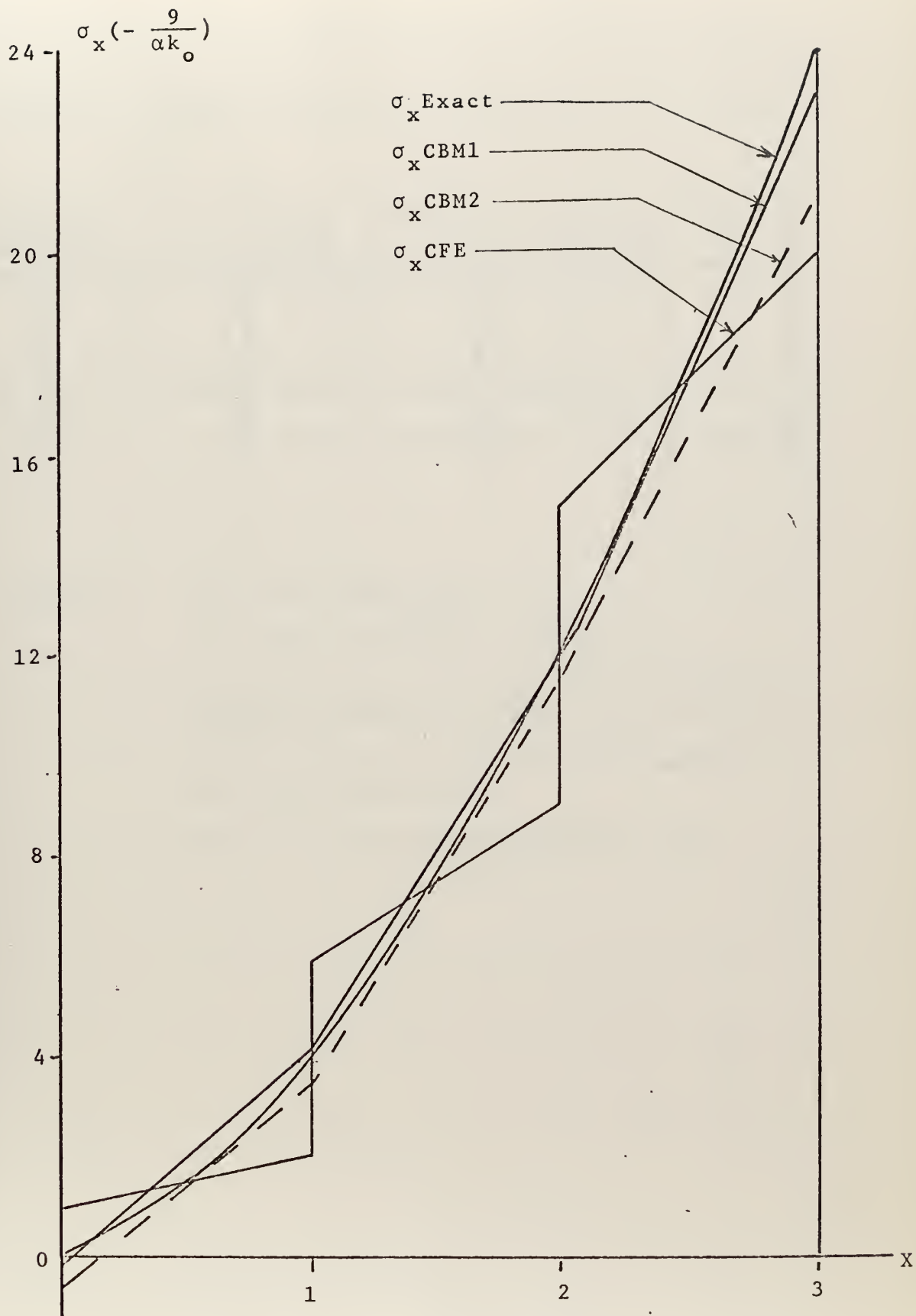


Figure 12. Exact Stress Distribution and Approximations to the Exact Stress.



TABLE I. Summary of Results for Problems III A1 and III A2.

$\sigma(x)$ x Exact	$\sigma(x)$ CBM1	Error %	$\sigma(x)$ CBM2	Error %	C.F.E.	$\sigma(x)$ C.Ave	Error %
0. 0	-0.33	-	-0.13	-	1	1	-
1. 4	3.43	14.25	4.26	6.5	2,6	4	0
2. 12	11.7	2.50	12.06	0.5	9,15	12	0
3. 24	23.6	1.66	21.46	10.58	20	20	16.67

- NOTES: 1.  $\sigma(x)$  CBM1 used known  $(x)$
2.  $\sigma(x)$  CBM2 used  $\frac{dU}{dx} = \text{constant}$
3.  $\sigma(x)$  C.F.E. is the conventional solution shown in Section III A1h
4.  $\sigma(x)$  C.Ave is the average at a node of the C.F.E solutions
5. Error % is  $\frac{\text{Exact}-\text{Approximate}}{\text{Exact}} \times 100$



Figure (12) shows three different approximations to the exact solution. The conjugate basis method with the exact stress distribution gave the best solution at node 4 and had the least mean square error throughout. The next best approximation was the conjugate basis method where the exact stress distribution was not known. The conventional finite element solution is also plotted.

### 3. Linear Displacement Model and Constant Properties

This is the same problem considered in the previous section only this time,  $k(x) = k_o = 1$ .

Equation (53) becomes

$$\sigma_N^e(x) = - \frac{\alpha k_o}{9} \int_0^L \frac{dU}{dx} \psi_N^e(x) dx \quad (56)$$

The nodal stresses are

$$\begin{aligned} \sigma_1^1 &= \sigma_2^1 = \frac{1}{2} \\ \sigma_1^2 &= \sigma_2^2 = \frac{3}{2} \\ \sigma_1^3 &= \sigma_2^3 = \frac{5}{2} \end{aligned} \quad (57)$$

The conjugate basis representation of the stress field is found using Equation (21) and is shown on Figure 13. The exact solution in this case is  $\sigma(x) = 2x$ . The conventional finite element solution is also shown. The factor  $-\frac{\alpha k_o}{9}$  has been disregarded.



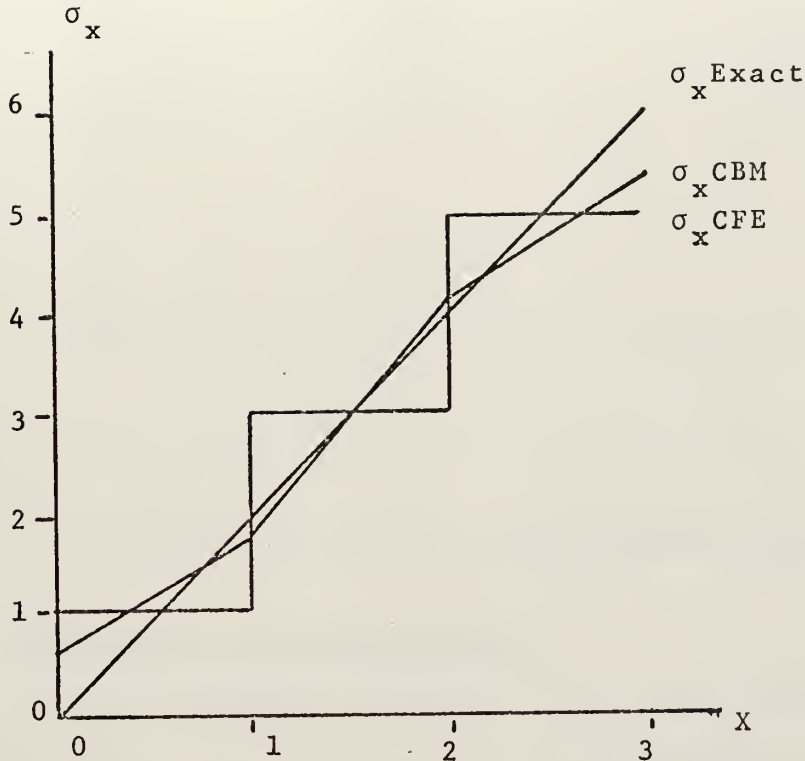


Figure 13.  $\sigma(x)$  vs  $x$  for  $k(x) = 1$ .

#### 4. Uniform Strain

Consider the same three element models with  $k(x) = 600$  to cancel the factors  $1/40$  and  $1/15$  resulting from the numerical calculations and  $U(x) = \frac{x}{10}$ . This is a case where node 4 is displaced 0.3 units along the  $x$  axis.

$\frac{dU(x)}{dx} = \text{constant} = .1$  In this case the exact solution, the conventional finite element solution, and the conjugate basis solution are exactly the same. This is shown in Figure 14. This problem corresponds to a uniform bar under a concentrated end load  $P = 30$ . (EA)





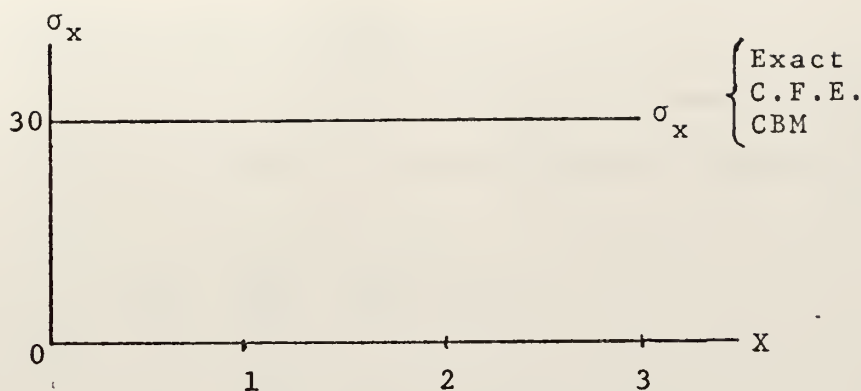


Figure 14.  $\sigma(x)$  vs  $x$  for Uniform Strain.

## 5. Discontinuous Displacement

In the previous examples, the stress was in fact continuous throughout the model. The CBM gave the best fit at the extremes and the least mean-square error over all. However, in problems where the stress is discontinuous due to a discontinuous displacement approximation, the CBM will not be the best fit. However, we consider examples with stress discontinuity to observe how the CBM tries to minimize the total error in a least squares sense in various models. The direct relation between discontinuous load and stress obtained here is true for the in-plane and bar problems. However, other problems in mechanics may have other stress-load relations. For example, for bending structures (beams or plates), discontinuous stress arises from discontinuous moment, and not discontinuous force.



a. Displacement at Node 3

For the same three-element bar given a displacement of 0.1 units at node 3, the displacement function is now

$$\begin{aligned} U(x) &= \frac{x}{20} & 0 \leq x \leq 1 \\ &= \frac{2}{20} & 1 \leq x \leq 3 \end{aligned} \quad (58)$$

The strain for elements one and two is a constant 0.05 and for element three is zero. The exact stress distribution is given by  $\sigma(x) = k(x) \frac{dU(x)}{dx}$  where  $k(x) = 600$ .

The conjugate nodal values are computed using Equation (23) and are shown below.

$$\begin{aligned} \tilde{\sigma}_1^1 &= \tilde{\sigma}_2^1 = \tilde{\sigma}_1^2 = \tilde{\sigma}_2^2 = \frac{600}{40} \\ \tilde{\sigma}_1^3 &= \tilde{\sigma}_2^3 = 0 \end{aligned} \quad (59)$$

The conjugate stress field is computed using Equation (21) and is shown on Figure 15 along with the exact and conventional solutions.



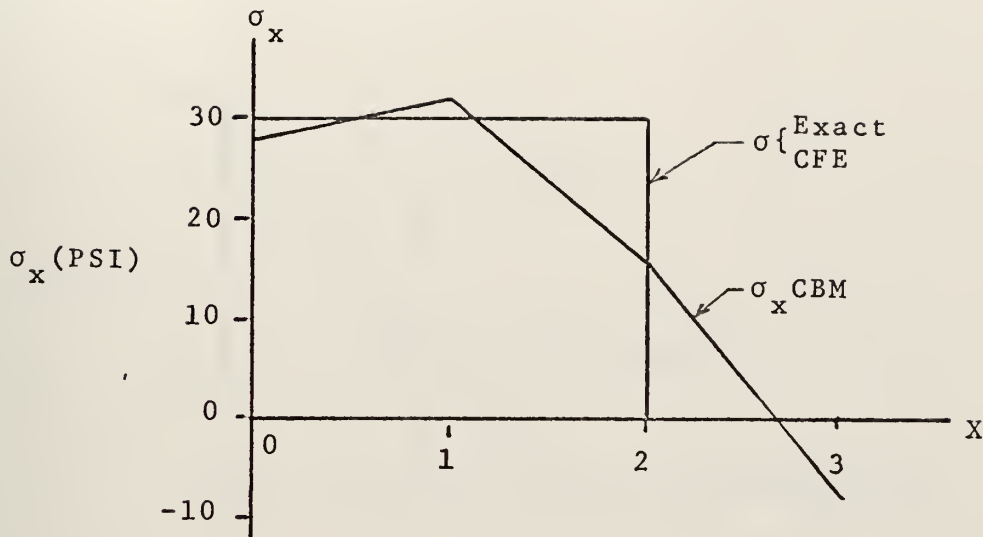


Figure 15.  $\sigma(x)$  vs  $x$  for Displacement at Node 3.

The conjugate basis method spreads the error throughout the model to obtain the best least squares fit, thereby giving a stress field in the element where there is no stress. Consider the area under the stress curve as a measure of the average error. For the exact solution  $A = 30 \times 2 = 60$  units; for the conjugate basis solution  $A = 60.4$  units. This gives a total percentage error of 0.66%. However, at node 3, the CBM value is only 53.3% of the maximum stress at that point. Clearly the conventional finite element method gives a better approximation.

#### b. Displacement at Node 2

If the model had been displaced from node 2 instead of node 3, the results would be similar in that the conventional constant strain element would be a better



approximation and the CBM spreads the error over the entire model. The results are shown below.

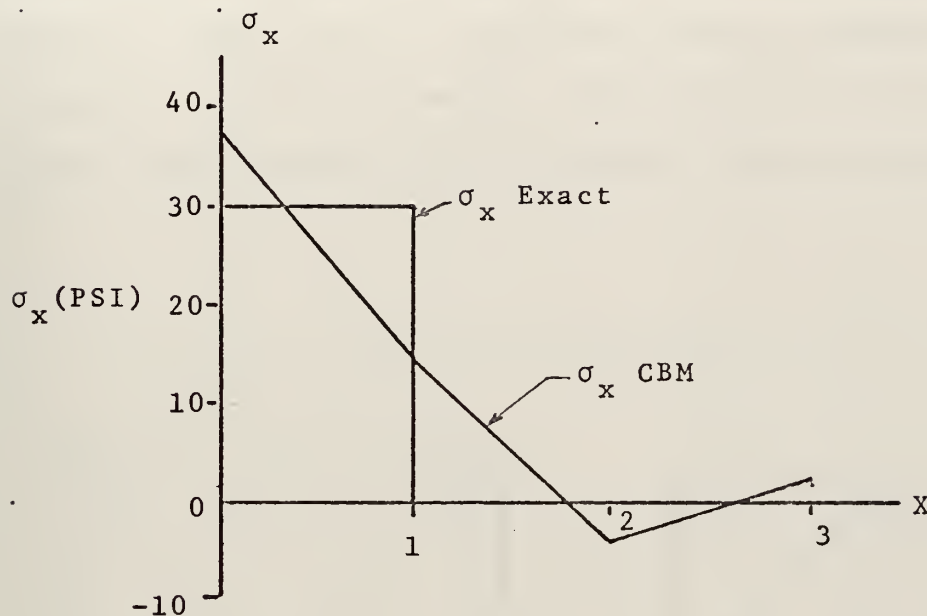


Figure 16.  $\sigma(x)$  vs  $x$  for Displacement at Node 2.

Again comparing the areas under the stress curves  $A(\text{exact}) = 30$ ;  $A(\text{CBM}) = 30.89$ . The error is 2.96% overall and 53.33% less than the maximum at node 2.

## B. TWO-DIMENSIONAL IN-PLANE PROBLEMS

The development of the computer program which was used to solve the two-dimensional in-plane problems is discussed in Section IV. Appendix B gives a description of the different finite elements which were used to obtain results to compare with the results obtained by the CBM. The computer program itself is listed in Appendix C.





The basic model used to verify the computer program was a 10 x 10 x 1 plane divided into either four or eight elements as shown below. The units used for numerical calculations are inches and pounds. The figure also shows the global node numbers and the element numbering system.

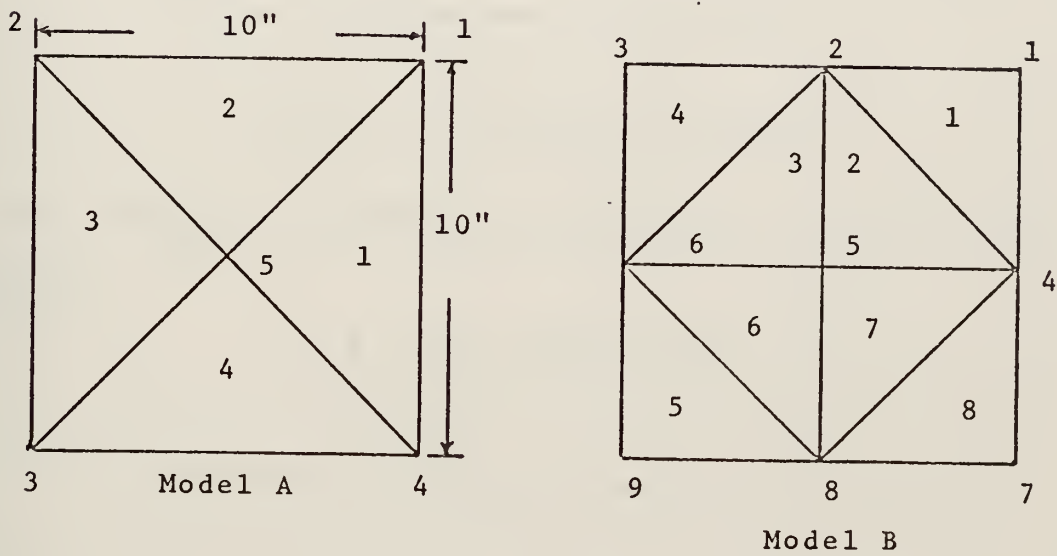


Figure 17. Typical Two-dimensional Models.

Each node has two degrees of freedom (DOF), which are in-plane displacements  $u$  and  $v$ , and for a typical node  $n$  they are numbered as shown below.



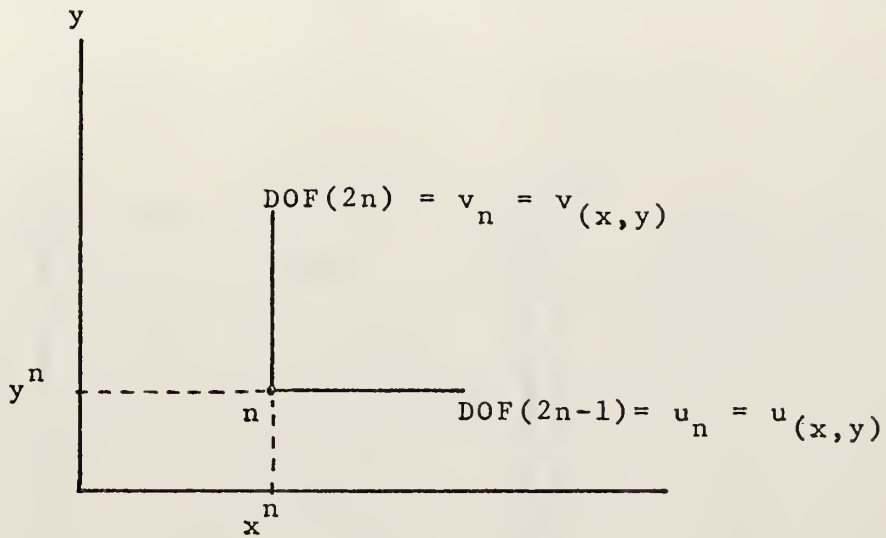


Figure 18. Reference System.

The following information is pertinent to all of the problems.

$$E = 30 \times 10^6 \text{ lbs/in}^2$$

$$\mu = 0.3$$

All stresses plotted are  $\sigma_x(x,y) \times 10^4 \text{ lbs/in}^2$



# 1. Model A with Uniform Edge Displacement

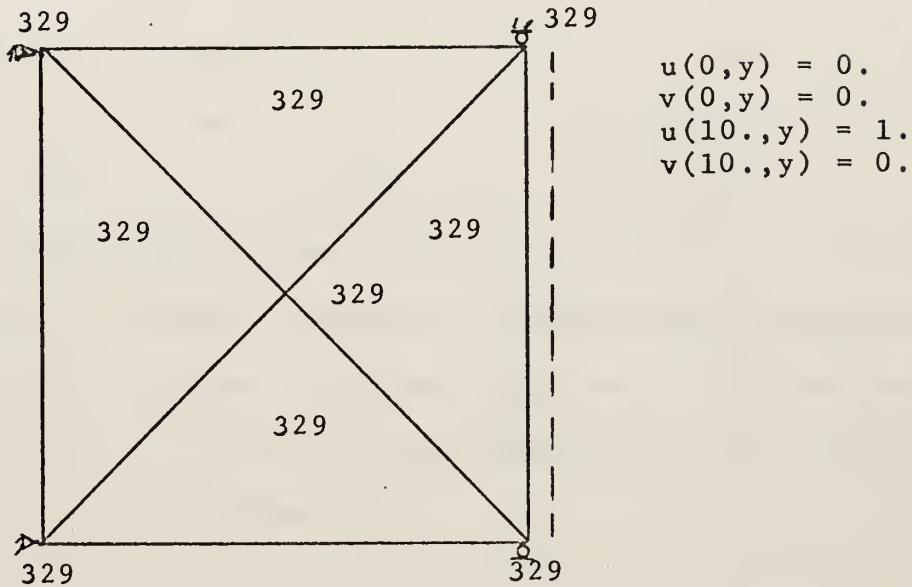


Figure 19.  $\sigma_x$  (PSI  $\times 10^4$ ) for Problem III B1.

The plane is prevented from displacement in the  $v$  direction; therefore  $\epsilon_y = 0$ . Equation (A-1) shows that the stress will be uniform across the model since the strain is uniform. This is the result that the CST solution gives. Because the CST solution is continuous for all elements, the conjugate basis solution cannot improve upon it. Both solutions in this case are exact for plane stress.

This problem is analogous to the three element bar which was displaced at node 4. See Section III A4. In the following figure, the stresses obtained by the conventional CST finite element solution are given in each element, while



the stresses obtained by the conjugate basis method (CBM) are the values given at the nodal points.

## 2. Model B with Uniform Edge Displacement

This problem is analogous to both the problem of the bar pulled uniformly at its end (III A4) and the first Model A plane problem (III B1). It confirms that mesh A was sufficient for the problem and that the CST is a sophisticated enough element for this type of problem. The difference in boundary conditions between this problem and problem III B1 accounts for the difference in stress values. In this case  $\epsilon_y < 0$ , that is contraction in the  $y$  direction is allowed, thereby reducing  $\sigma_x$ .

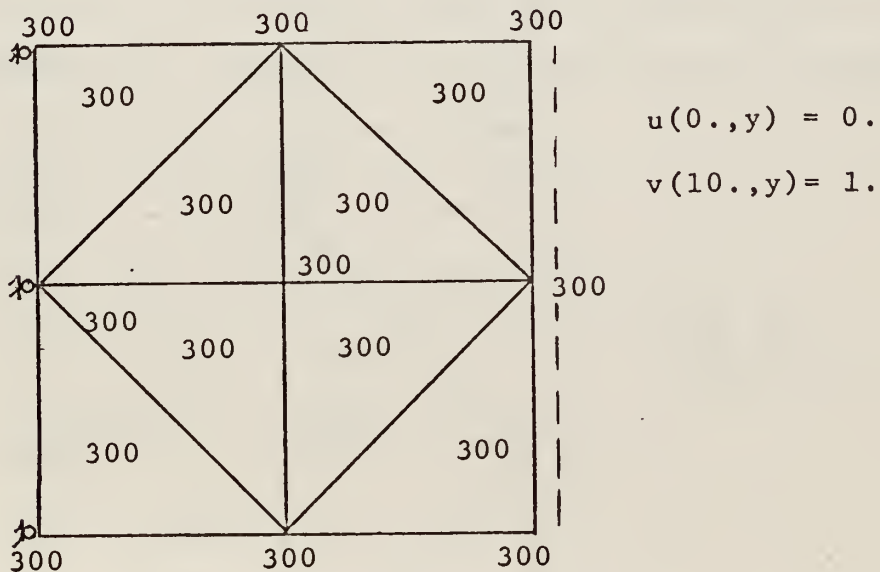


Figure 20.  $\sigma_x$  (PSI  $\times 10^4$ ) for Problem III B2.





### 3. Model B with Uniform Edge Displacement, Modified

Analytical values of  $\sigma_x$  were calculated for  $x = x(10,y)$ ,  $x = x(5,y)$  and  $x = x(0,y)$  using the plane stress equations (A-1). The values of strain were approximated by dividing the total contraction in the  $v$  direction for a given  $y$  by the original length 10. The strain  $\epsilon_y$  was considered constant along a constant  $y$ . The displacements were calculated in the CST routine.

The values of  $\sigma_x$  calculated were

$$\sigma_x(0.) = 329 \quad \sigma_x(5.) = 292 \quad \sigma_x(10.) = 300$$

For  $x = 0$  and  $x = 5$  the CBM gives the better approximation. At  $x = 10$  the difference in percentage of error between the CST solution and the CBM is less than 0.67%. It is also interesting to note that the average of the CST values at nodes 2 or 8 is the same as the CBM value. This gives mathematical substance to the engineering practice of using the average value at a node.

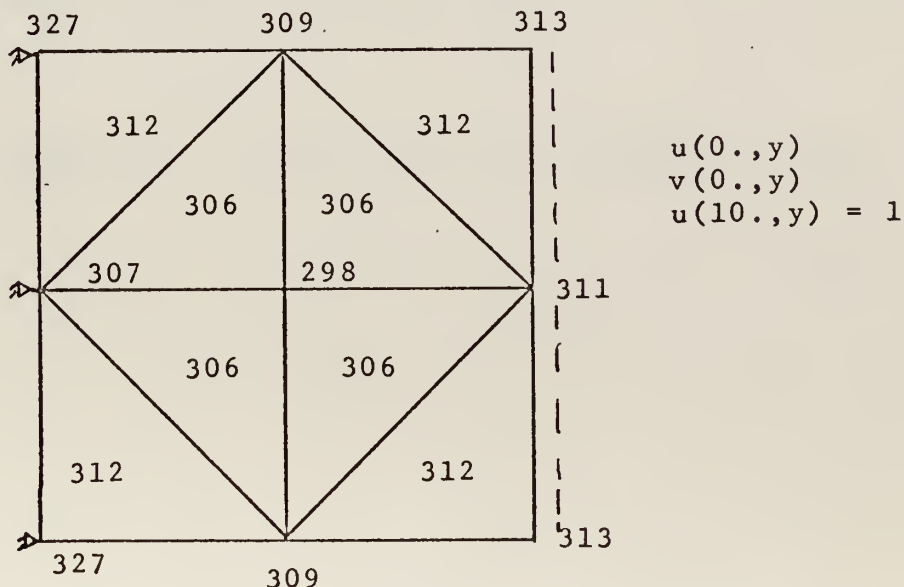


Figure 21.  $\sigma_x$  (PSI x 10<sup>4</sup>) for Problem III B3.



#### 4. Model A with Linear Edge Displacement

Here the right edge is given a linear displacement as shown below. Using the analytical procedure discussed in Problem III B3, the values of  $\sigma_x$  range from  $329 \times 10^4$  along the edge  $(x,10)$  to zero along the edge  $(x,0)$ . The CBM values are the best continuous approximation available for this model. A plot of  $\sigma_x(0)$  vs  $y$  along  $(0,y)$  shows how the CBM is better in approximating the maximum value.

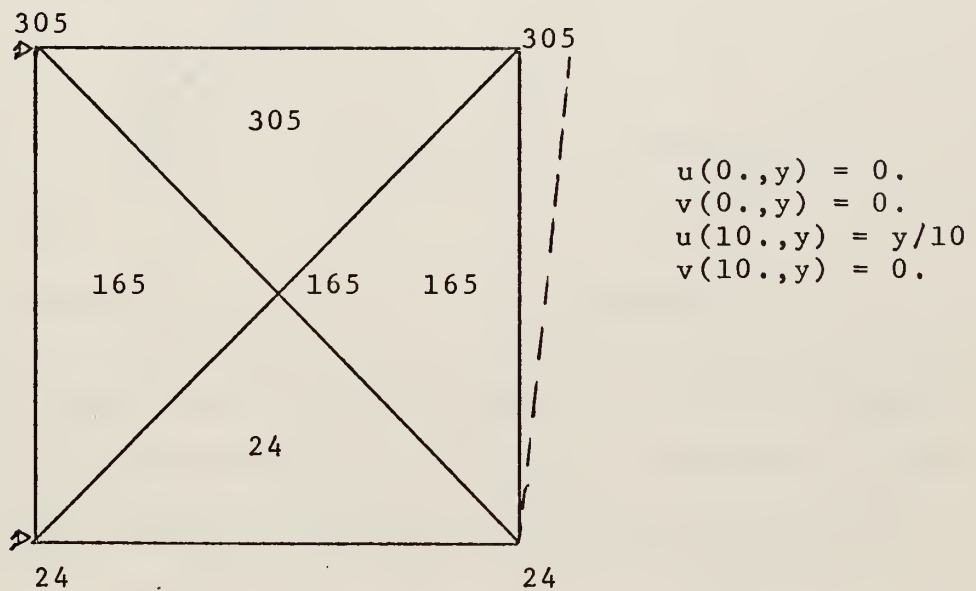


Figure 22.  $\sigma_x(\text{PSI} \times 10^4)$  for Problem III B4.



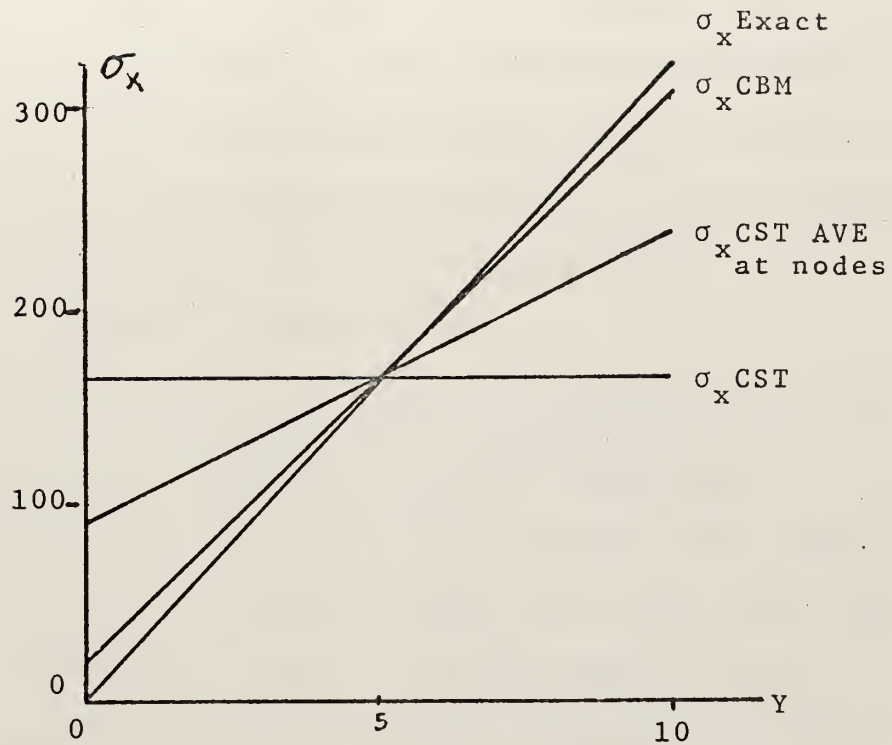


Figure 23.  $\sigma_x(0)$  vs  $y$  for Problem III B4.

A comparison of the percentage of error at  $(x,y) = (0., 10.)$  that the CBM value is 7.4% too low while the CST average value is 28.5% low and the minimum CST value is 50% low.

##### 5. Model B with Linear Edge Displacement

The applied displacements in this problem make it similar to Problem III B4; however, the other boundary conditions in this problem allow for movement in the  $v$  direction. In part the displacement solution of the CST program shows that at  $x=0.$ ,  $x=5.$ , and  $x=10.$ ,  $\epsilon_y < 0.$  Therefore, along the bottom edge where  $\epsilon_x$  is very small, the effect of  $\epsilon_y$  becomes dominant and a negative  $\sigma_x$  results.



From the results of the CST displacement solution, the value of  $\epsilon_x = \frac{\partial u}{\partial x}$  along the edge (x,0.) is 0.0026 and the value of  $\epsilon_y = \frac{\partial v}{\partial y} = 0.016$  along x=10. and 0.015 along (5,y) and (0,y). Using these values of  $\epsilon_x$  and the average of the  $\epsilon_y$ 's in Equation (A-1) for stress yields

$$\sigma_x(x,0) = -73 \times 10^3 \text{ PSI}$$

The CST solution is attempting to reflect this in elements 5 and 8. The CBM does show the compressive stresses and of course is continuous throughout the model. The average of the CST values at nodes where more than one element are incident is close to the CBM value at that node. For example, at node 5 the CST average is 150 and the CBM value is 148. This again confirms the existing practice of averaging.

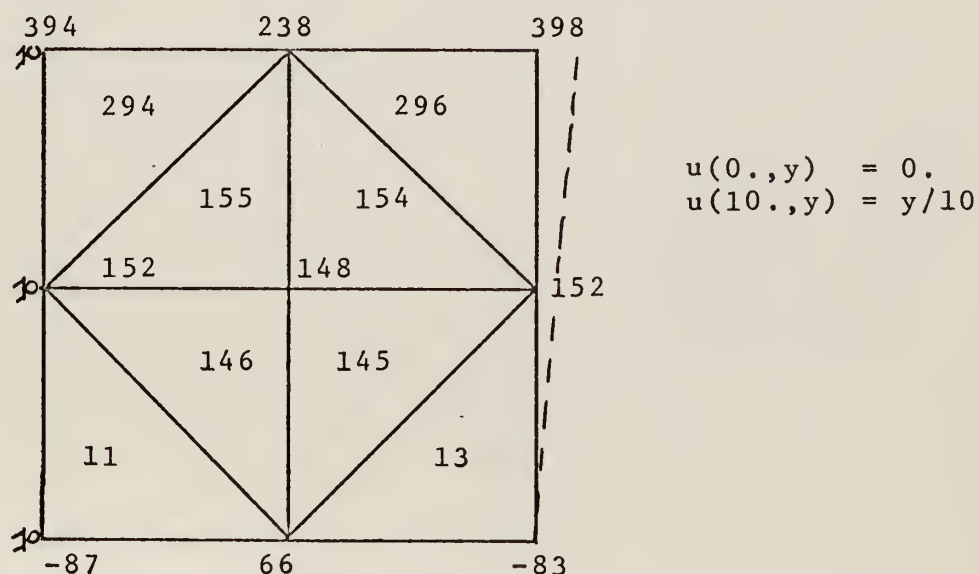


Figure 24.  $\sigma_x$  (PSI  $\times 10^4$ ) for Problem III B5.





## 6. Model B With Piecewise Linear Edge Displacement

This problem has boundary conditions similar to problem III B 4; but, since it has two elements along  $x = x(10,y)$  and the applied displacement is only at node 1, the displacement profile of the edge is only piecewise linear with discontinuous slope.

The expected stress profile is greatest at  $(x,10)$  where  $\epsilon_x$  is maximum and compressive at  $(x,0)$  where  $\epsilon_x=0$  but a compressive  $\epsilon_y$  exists. Likewise  $\epsilon_x$  is higher along  $(0,y)$  because  $\epsilon_y=0$ , than along  $(5,y)$ .

The CBM values conform with the expected distribution and give a continuous stress field which is the best approximation in this case.

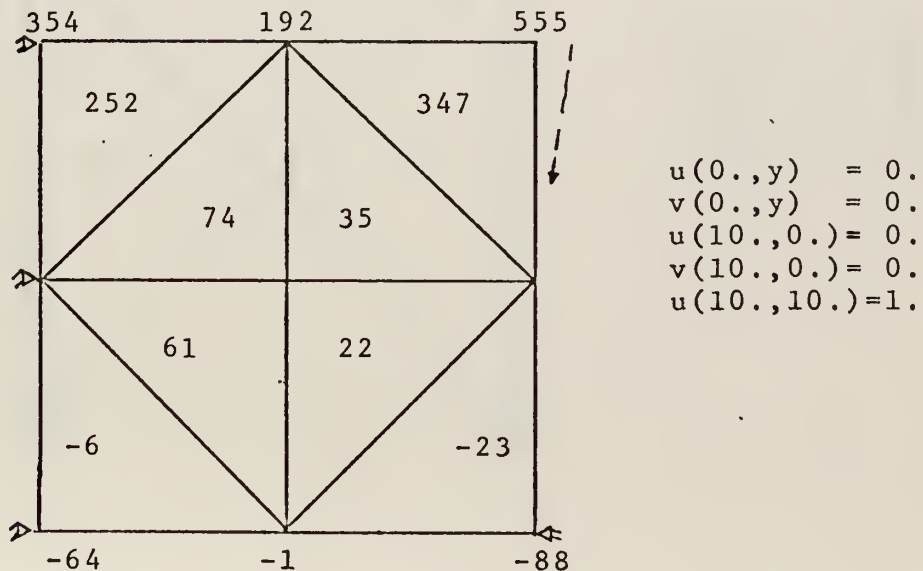


Figure 25.  $\sigma_x$  (PSI  $\times 10^4$ ) for Problem III B6.

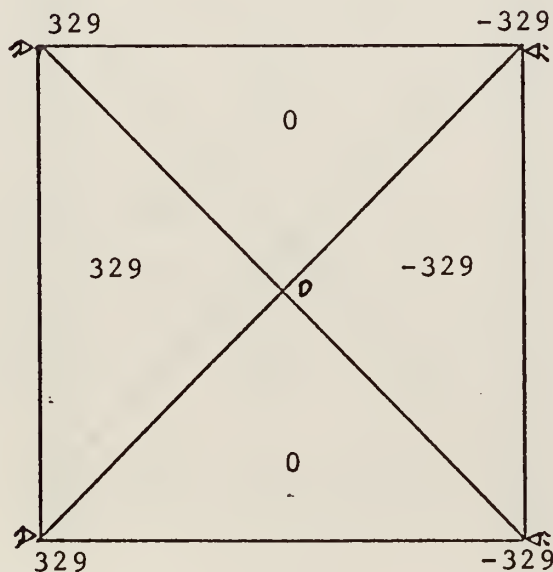


## 7. Model A With Center Node Displacement

For this problem the stress is discontinuous due to the displacement of node 5 in the interior of the model. The CST solution gives an exact representation of the stress field. Element 1 is in compression and element 3 is in tension.

The CBM values are exact at the nodes. A stress plane constructed linearly thru the nodes would be in error at all locations other than the nodes.

If a three dimensional plot is made with stress as the vertical axis, the volume under the CST plot would equal the volume under the CBM plot at  $25 \times \sigma_{\max}$ .



$$\begin{aligned} u(0.,y) &= 0. \\ v(0.,y) &= 0. \\ u(10.,y) &= 0. \\ v(10.,y) &= 0. \\ u(5.,5.) &= 0.5 \end{aligned}$$

Figure 26.  $\sigma_x$  (PSI  $\times 10^4$ ) for Problem III B7.



### 8. Model A With Center Node Displacement, Modified

The model is subject to a discontinuous stress field due to the internal displacement of the center node. If the model allowed more flexibility, one would expect the stress to be discontinuous in the region of node 5 and continuous along the edges. The CBM does not show the abrupt change at node 5 but does approximate the solution expected of a more flexible and hence more accurate model.

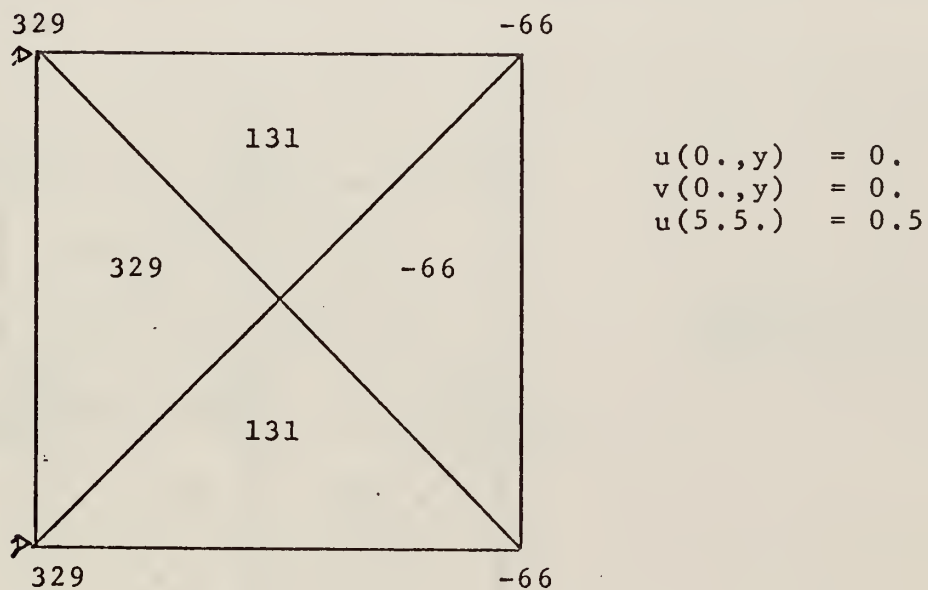


Figure 27.  $\sigma_x$  (PSI  $\times 10^4$ ) for Problem III B8



## 9. Model B With Center Node Displacement

This problem is similar to the previous problem on model A with the exception that the boundary conditions on this problem allow displacements in the  $v$  direction. The stress is discontinuous in the region around the center node, node 5. However it is unlikely that the stress is as severely discontinuous as the CST solution indicates in this region. Intuitively  $\sigma_x$  has a maximum tensile value at (0,5) and a maximum compressive value at (10,5) and decreases in absolute value away from the line of action of the displacement.

For this model, subject to a point discontinuity, the CBM gives a better overall representation of the stress field.

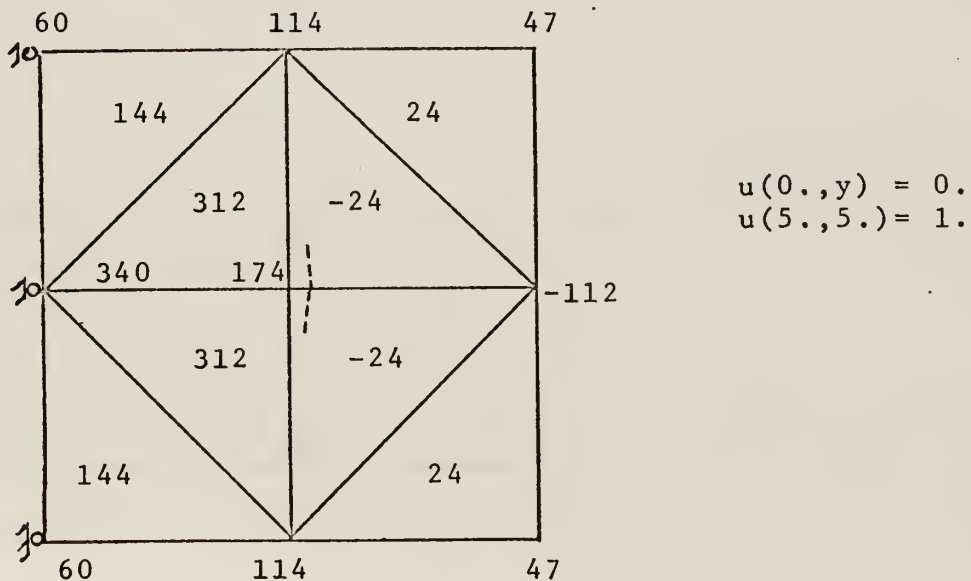


Figure 28.  $\sigma_x$  (PSI  $\times 10^4$ ) for Problem III B9





# 10. Model B With Uniform Centerline Displacement

This is another problem with a discontinuous stress resulting from an internal displacement. Note that to minimize deflection in the  $v$  direction, the boundary condition  $v(5,5) = 0$  has been imposed.

The expected value of  $\sigma_x(x)$  for  $x > 5$  is zero. The CST solution is superior from two standpoints. It reflects the stress discontinuity very well and it gives a better approximation to the stress field over the right half of the model. It is interesting to note that the average CST value at nodes 2 and 8 is the CBM value.

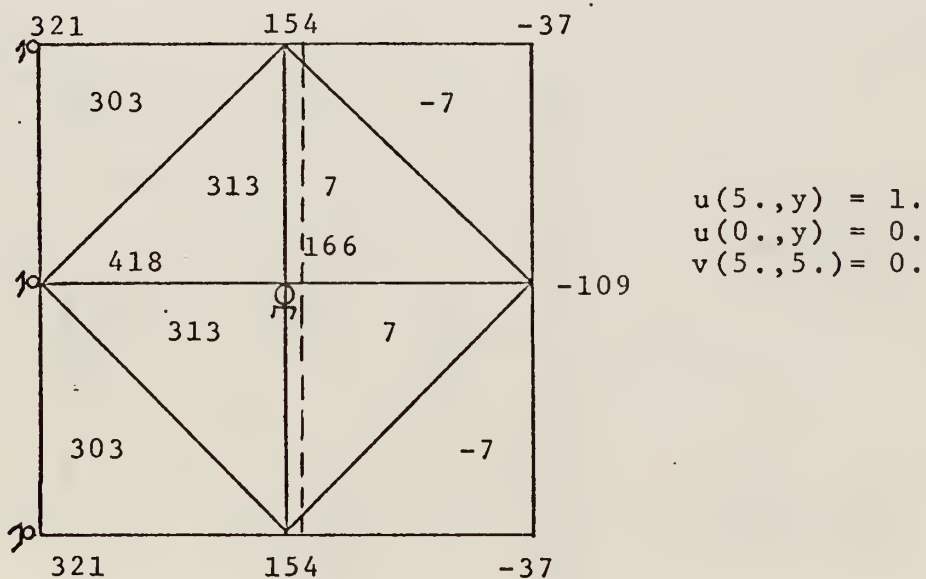


Figure 29.  $\sigma_x$  (PSI  $\times 10^4$ ) for Problem III B10



### 11. Model B Modified, With Uniform Centerline Displacement

This mesh is a modification of model B and was designed to determine how rapidly the CBM stress would converge to zero. Each node along  $x=5$  and  $x=10$  was displaced an equal amount to force rigid body motion.

The CST model responds to the discontinuity quickly as expected. The CBM does try to converge and is a better approximation over this part of the model than the approximation with the previous mesh (III.B.10). The conclusion is that if a discontinuity occurs across an entire model, and there is sufficient room for the continuous function to correct itself, and the area of interest is not at the discontinuity, the CBM will be the best approximation for a continuous field.

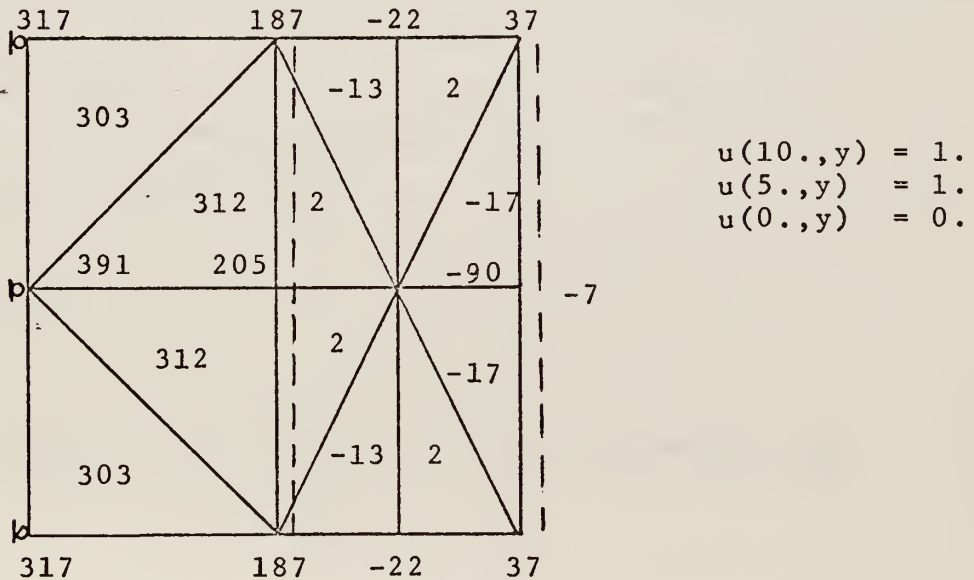


Figure 30.  $\sigma_x$  (PSI  $\times 10^4$ ) for Problem III B11



## 12. Model B Tapered With Uniform Edge Displacement

This model is another modification to model B. The length has been doubled and a taper introduced by making the right edge one half the height of the left edge. Symmetry about the horizontal centerline has been maintained. The model simulates a tapered plane and is the two dimensional analog of the one dimensional tapered bar. Both the CST solution and the CBM give the expected stress distribution. However the CBM is continuous over the entire model and therefore is a better approximation.

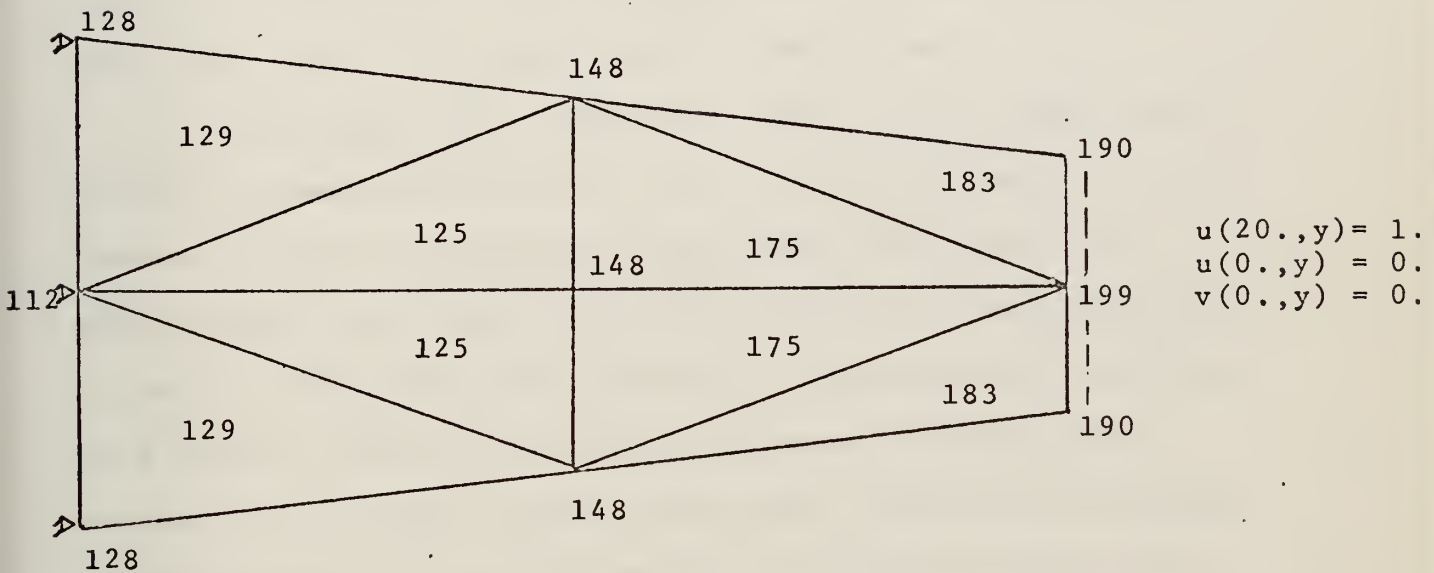


Figure 31.  $\sigma_x$  (PSI  $\times 10^4$ ) for Problem III B12



### 13. Composite Material Models With Uniform Edge Displacement

This problem consists of using the CBM with a CST input on the composite material models used by Lin, Salinas, and Ito [Ref. 6] and comparing the results for stress convergence and computer time usage. The models used in Ref. 6 are shown in figures (32) and (33). The PLISOP model shown in figure 34 has been used by Salinas subsequent to publishing Ref. 6. The stresses resulting from using the CST and LST routines on figures (32) and (33) and the PLISOP routine in figure (34) (see Appendix B) are shown on figures (35, (36), and (37) along with the CBM values.

In figure (37), along the edge (5.2,y), where there is only one material present, the CBM yields a smooth curve. However, where two materials are present and there is a sharp change in stress due to the different Young's Modulus of the two materials, the CBM tries to smooth out the change in a manner similar to the discontinuous problems shown earlier. As a result several CBM model values in the region of the change in material are not in agreement with values obtained from the other solutions. The results are in good agreement away from this area of change.

An analysis of the amount of computer time each program used is shown in Table II.





	MODEL 3 (124 DOF)	MODEL 4 (242 DOF)	LST MODEL 3 (430 DOF)	PLISOP 16 ELEMENTS (204 DOF)
FORM GFM	0.12	0.13		
INVERT GFM	20.17	133.11		
CALCULATE STRESS	<u>3.93</u>	<u>14.11</u>		
SUBTOTAL FOR CBM	24.22	147.35		
CPU TIME	34.85	165.23		64.72
TOTAL FOR 1 RUN	57.83	185.38	232	88.70

TABLE II

Comparison of CBM Computer Time in Seconds With LST and PLISOP Time Usage for  
Similar Problems



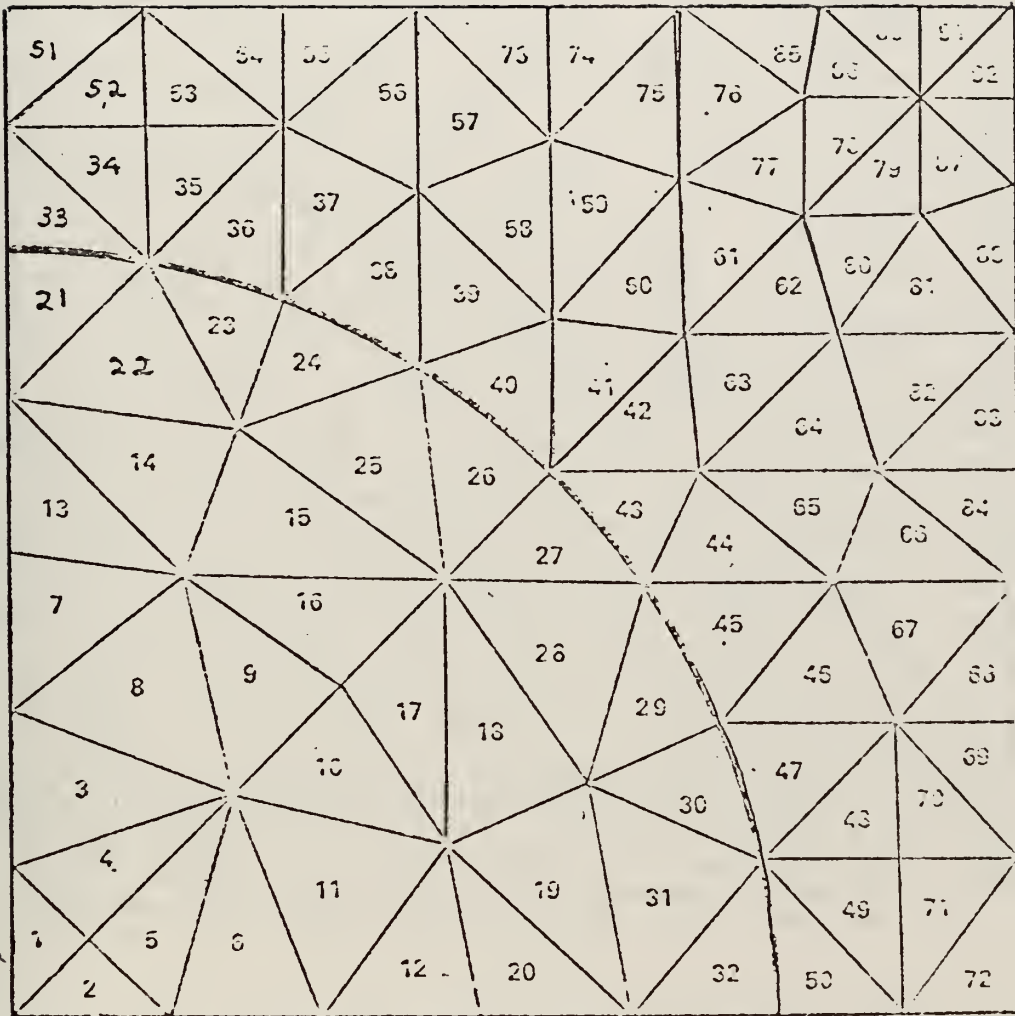


Figure 32. Finite Element Grid System, 124 DOF.



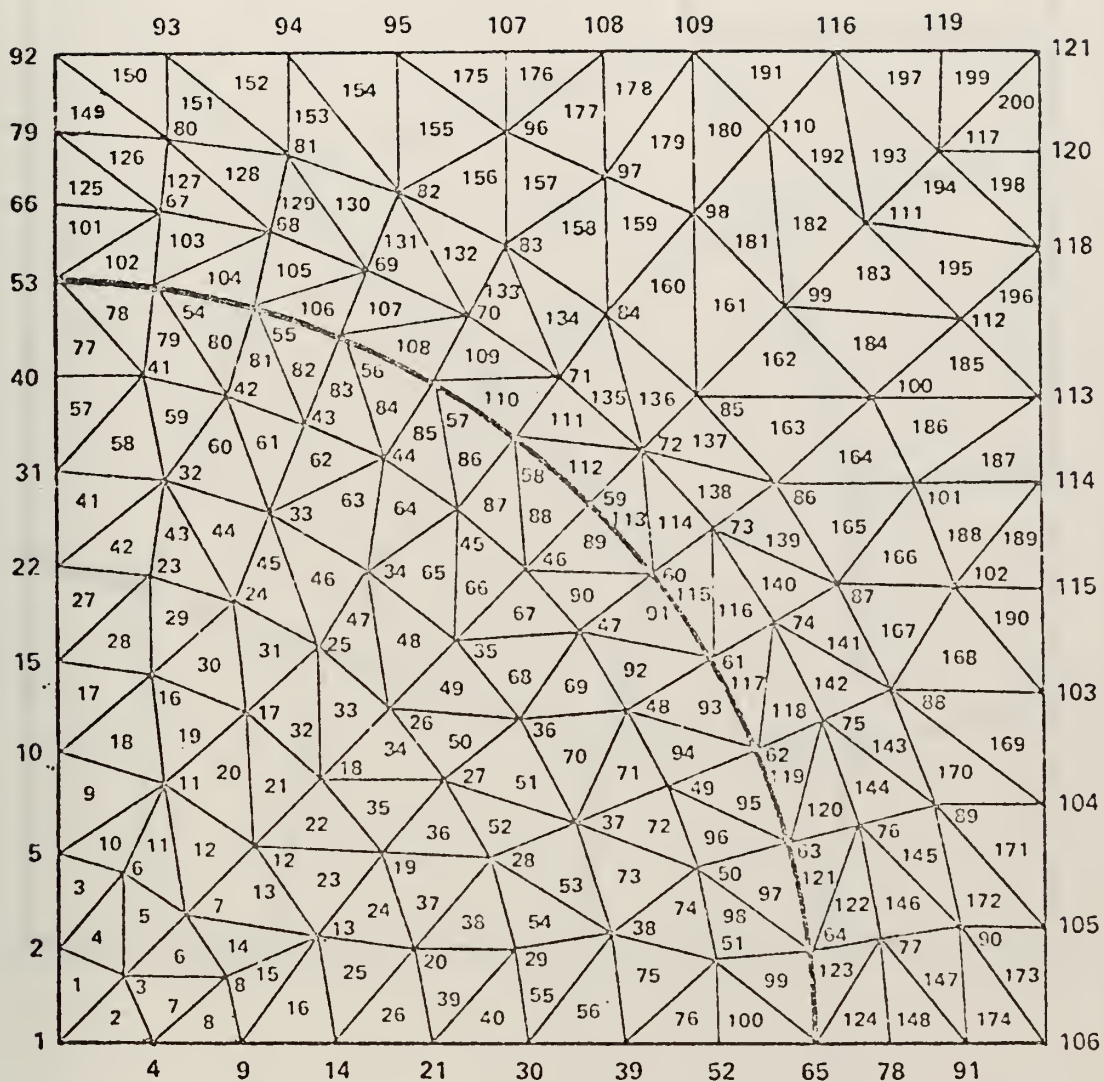


Figure 33. Finite Element Grid System 242, DOF.



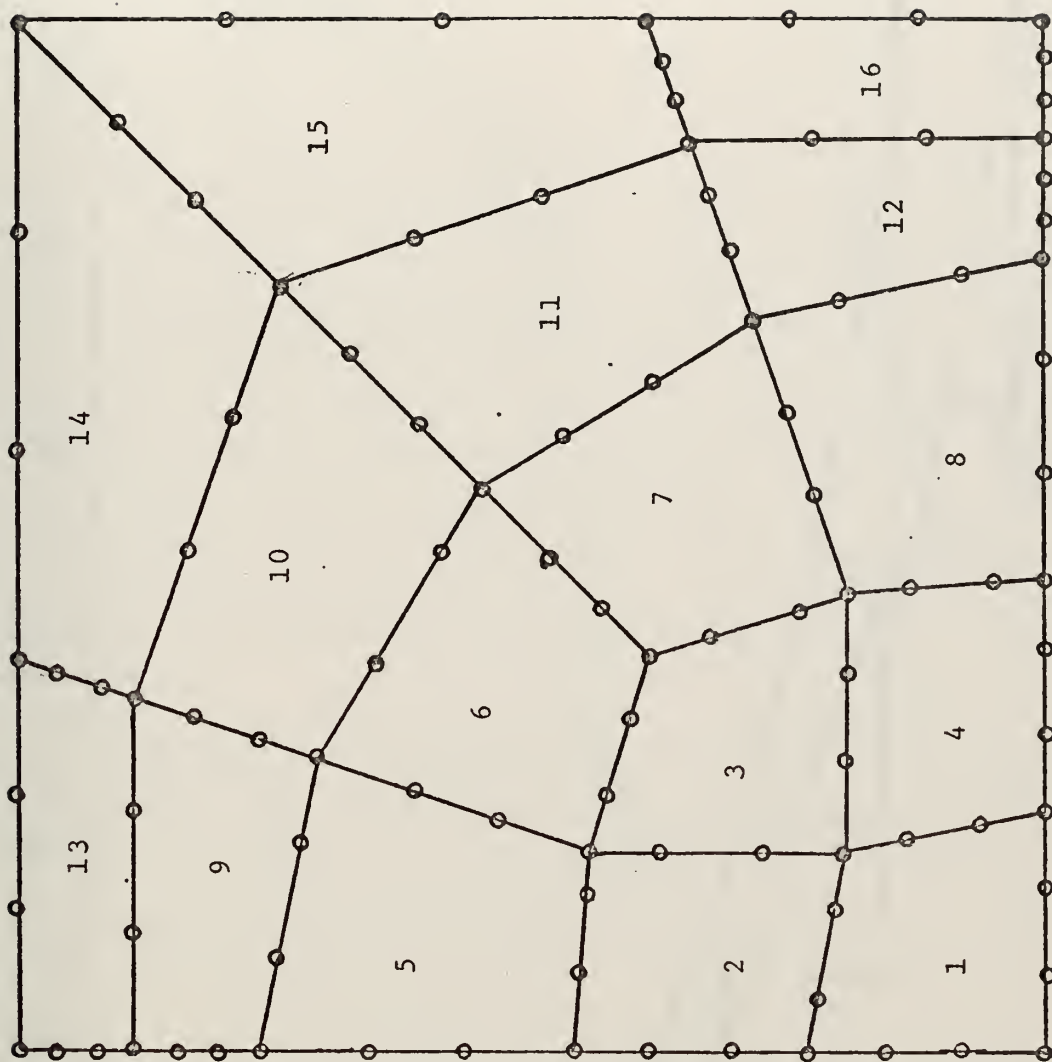


Figure 34. Finite Element Grid System for PLISOP, 204 DOF.





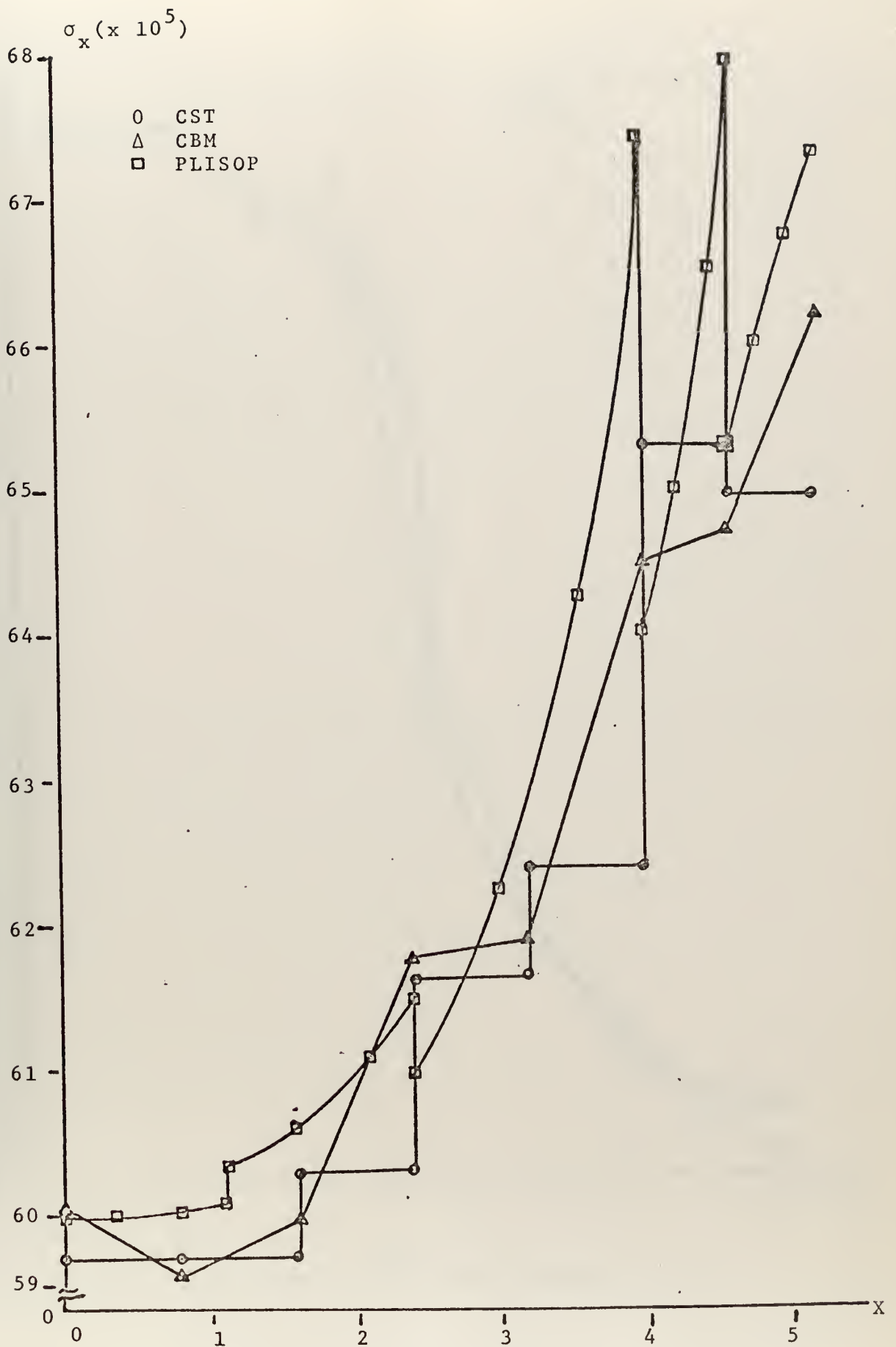


Figure 35.  $(x, 0.) (PSI \times 10^5)$  for Problem III B13.



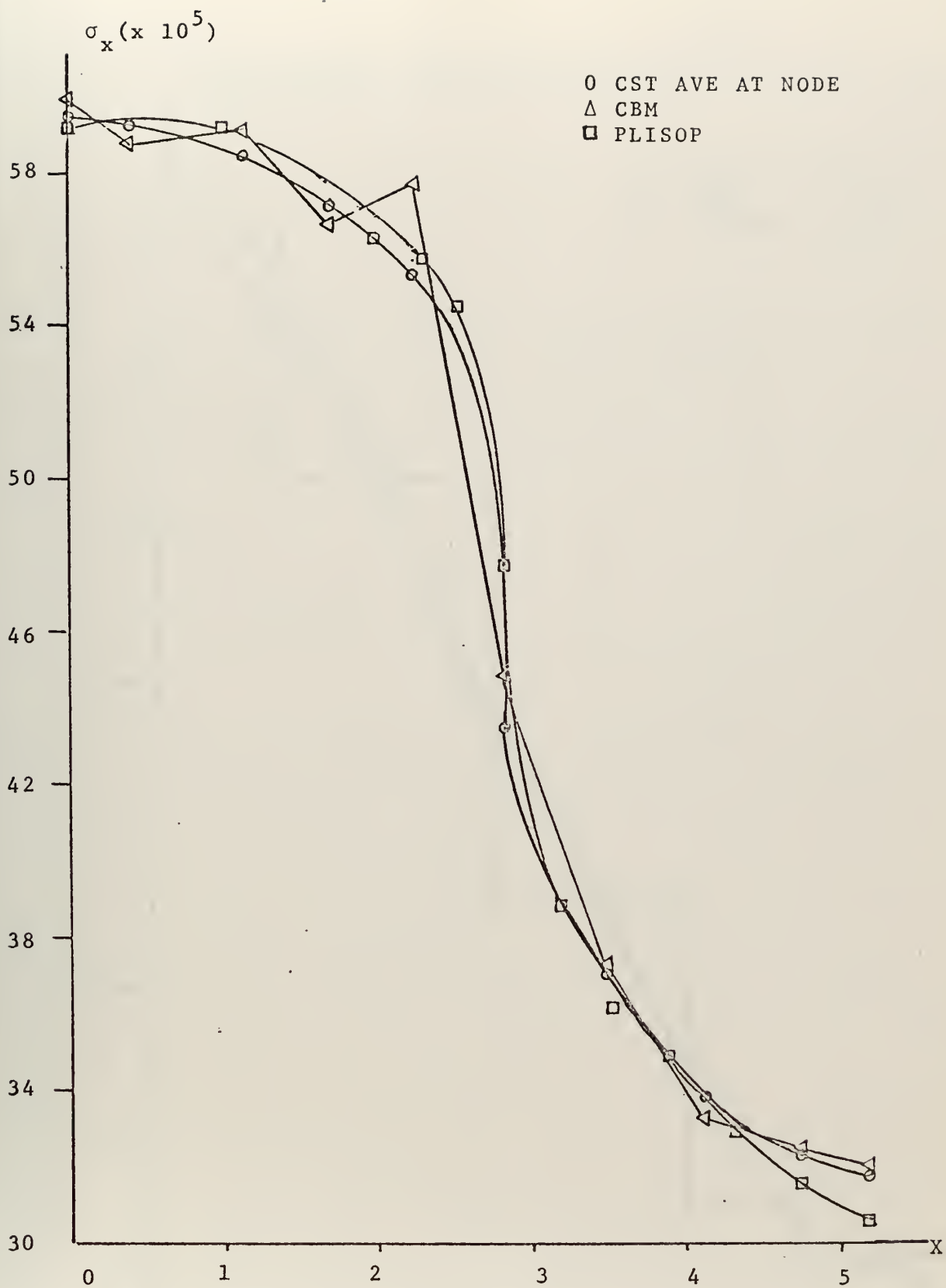


Figure 36.  $\sigma_x(x=y)(\text{PSI} \times 10^5)$  for Problem III B13.



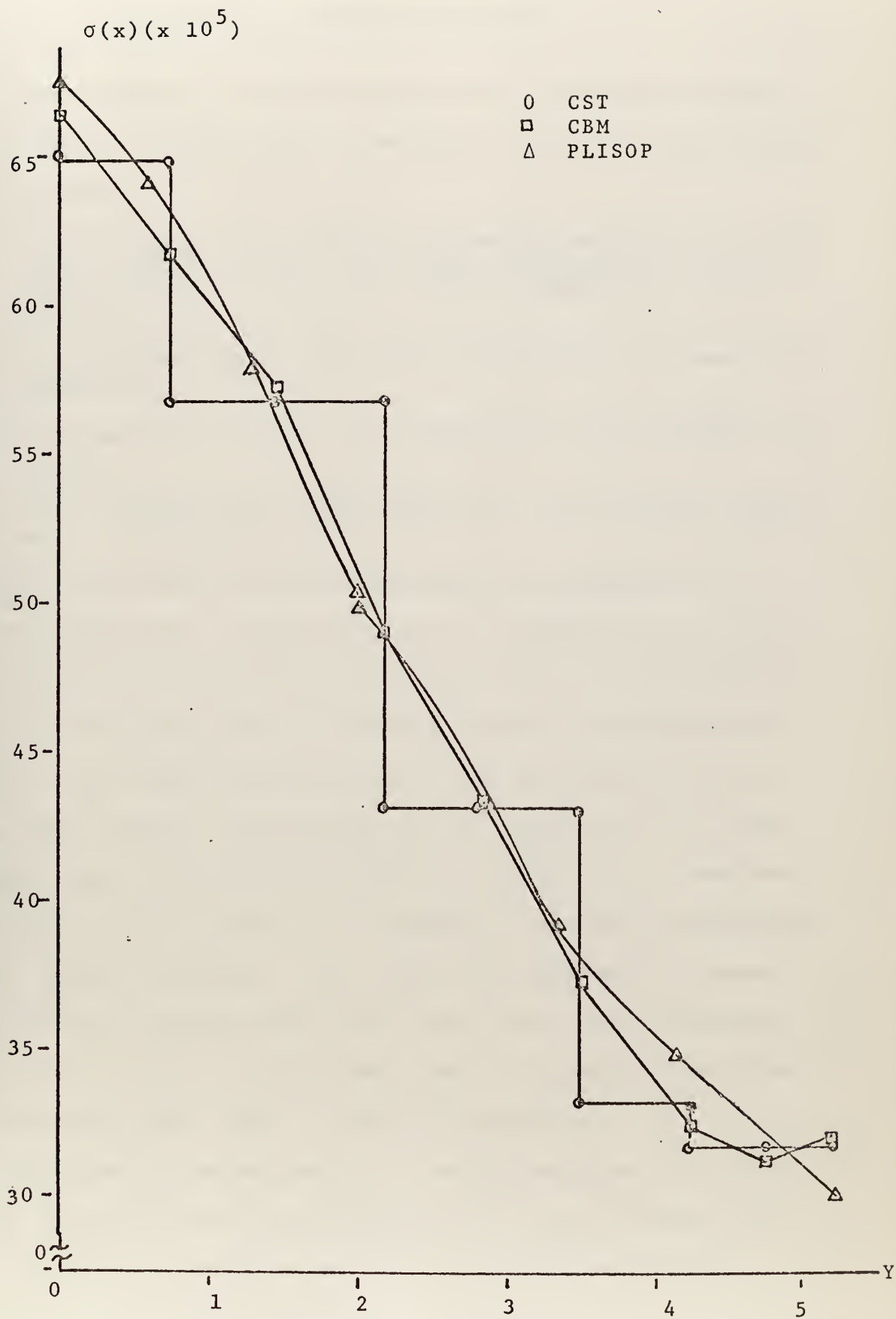


Figure 37.  $\sigma_x(5.2, y) (\text{PSI} \times 10^5)$  for Problem III B13.



#### IV. THE COMPUTER PROGRAM DEVELOPMENT

In developing a computer program to determine stresses utilizing the conjugate basis method, four major requirements had to be met:

- i. The inverse of the global fundamental matrix is needed. This requires forming the element fundamental matrices and merging them into the global fundamental matrix itself.
- ii. An' approximation to the stress field in the element is required.
- iii. The conjugate nodal stress values for each element are formed.
- iv. The conjugate basis approximation to the stress field must be assembled.

There are many existing programs which satisfy the second requirement. In this thesis a program utilizing the CST written for use in Ref. 6 has been used. It was chosen because it was available; it uses a simple two-dimensional element — the three noded triangle; and problem solutions using this element were available for comparison as to the computer time used and the accuracy of results. It was not an objective of the thesis to develop an optimum conventional finite element solution. Any other CST program or a more sophisticated program could have been used. The advantage of the CBM is that it makes the stress at a node a function of the entire model and not just the element.

Therefore the development of the CST program itself will not be discussed with the exception of a brief comment on the constitutive relation matrix,  $C$ . For plane stress





problems where  $\sigma_z = \tau_{xz} = \tau_{yz} = 0$

$$C = \frac{E}{1 - \mu^2} \begin{bmatrix} 1 & \mu & 0 \\ \mu & 1 & 0 \\ 0 & 0 & .5(1-\mu) \end{bmatrix}$$

where  $\{\sigma\} = [C]\{e\}$  .

For the CST, each displacement field is approximated by a linear field over each element, hence the local basis functions are area coordinates. The local fundamental matrix, which is the inner product of each of the basis functions, is therefore dependent on the total area of each element. The integration can be found in Felippa [Ref. 7] and the resulting matrix is

$$\frac{A}{12} \begin{bmatrix} 2 & 1 & 1 \\ 1 & 2 & 1 \\ 1 & 1 & 2 \end{bmatrix}$$

After the area of each element is calculated in the normal CST routine, the element fundamental matrix - EFM - is formed. It is immediately merged into the global fundamental matrix - GFM. The merging routine is described in section III.A.1.d.

After the entire GFM is formed, it is inverted using subroutine SYINV. This is the most time consuming addition to the CST program. See Table II. Notice that for the 92 element model SYINV used 20 seconds but for the 200 element model the time was 133 seconds.



The conjugate basis nodal stresses are calculated in two steps at the completion of the standard CST program. The assumption is made that stresses will only be calculate at nodes. Since  $\phi_{\Delta} = 1$  at a node (see section II.C. and section III.A.1.e.) the values of the local conjugate basis function at a node are just elements of the GFM inverse, in accordance with equation (44). This assumption is not a serious limitation because the finite element mesh can be arranged to have a node at any point of interest or the stress can be calculated by interpolating between neighboring nodes. However it greatly simplifies the computer calculations.

Recall that the conjugate nodal values of stress for each element are given by Eq. (23) as

$$\sigma_N^e = \int_0^L \sigma(x) \psi_N^e(x) dx$$

The CST value of  $\sigma(x)$  is constant for each element and is taken from the CST solution. The solution of  $\int_0^L \psi_N^e(x) dx$  is found in Ref. 7 and is  $\frac{A(e)}{3}$  for each N. Therefore the conjugate value for each node of element e is  $\frac{A(e)}{3} \sigma(e)$ .

$$\sigma_N^e = \frac{A(e)}{3} \sigma(e) \quad (60)$$

The conjugate function representation of stress is given by Eq. (21) as

$$\sigma(x) = \sum_{e=1}^E \sigma_N^e \psi_e^N(x)$$



In the computer program  $\sigma(x)$  is calculated one node at a time. The value of  $\sigma_N^e$  is multiplied by the element of the GFM inverse in the row corresponding to the global node that the local node N is incident to and the column corresponding to the global node being calculated. This multiplication is carried out for each element and the resulting sum is printed out as the nodal stress.

The modification of an existing conventional finite element program to perform conjugate basis calculation of stress requires the addition of three simple algorithms.

- i. An algorithm which forms the global fundamental matrix (GFM). This algorithm may be located in the element stiffness DO loop, where the element fundamental matrices (EFM) are individually formed and whose elements are inserted in the appropriate place in the global fundamental matrix,  $C_{\Delta\Gamma}$ .
- ii. An algorithm to invert the global fundamental matrix  $C_{\Delta\Gamma}$  and obtain  $C^{\Delta\Gamma}$  (see equation (12)).  $C_{\Delta\Gamma}$  is a banded symmetric matrix and inversion algorithms are available. (In this work E. Wilson's SYINV subroutine was used.) This algorithm is located after  $C_{\Delta\Gamma}$  is formed, and is the most time consuming aspect of the conjugate basis method.
- iii. An algorithm for the calculation of nodal stresses associated with equations of the conjugate basis method. This algorithm uses the conventional stresses of the finite element method and must therefore follow the conventional stress calculation routine.



A listing of a CST finite element routine is given in Appendix C with the CBM modifications shown enclosed in boxes.





## V. CONCLUSIONS AND RECOMMENDATIONS

As a result of this study several conclusions can be made concerning the use of conjugate basis functions with in-plane problems.

Where the model is not subject to interval discontinuities, the CBM gives the most accurate approximation to the stress over the entire model for a given displacement.

If there is a point or localized discontinuity, the CBM will be a poor representation of the stress near the disturbance but will be a good approximation away from the disturbance. Mesh refinement can localize the disturbed area. It is understood that points of stress discontinuity are usually points of interest and that mesh refinements generally increase computer time, therefore the use of the CBM is limited.

If there is a stress discontinuity across the entire model, the CBM is a poor choice if the model is too small or too coarse to allow the CBM to settle out. Refining the mesh may be worthwhile if a continuous approximation to the stress is wanted in regions away from the discontinuity. However the additional computer time needed places a premium on this marginal gain.

If a large number of problems are run on the same model and the global fundamental matrix can be inverted once and stored, the additional computer time per problem for the CBM solution is minimal. The advantage of a continuous



stress solution can be had without using the more sophisticated elements with nodal strain degrees of freedom.

Finally, at nodes where the stress should be continuous and several elements were incident at that node, the average of the CST stress values at that node agreed very closely with the CBM stress value. This gives mathematical substantiation to an engineering practice.

It is recommended that

1. The CBM be used for in plane problems without interval discontinuities because the resulting stress field will be continuous, which the actual stress field is, and the stresses will be consistent with the displacements.
2. Further studies with the CBM should be carried out on other classes of problems. For example, plate problems or beam problems might be better approximated with CBM solutions.
3. Additional studies be carried out to determine the cost effectiveness of incorporating and using the conjugate basis method in existing conventional finite element programs.
4. An investigation be undertaken to determine if the CBM can be modified to yield stress discontinuity when appropriate.
5. A study be made to establish the relation of domain modeling to CBM analysis.



# APPENDIX A

## THE IN-PLANE PROBLEM

In this discussion a plane is defined as a body bounded by two surfaces of zero curvature whose thickness,  $h$ , is much less than its surface dimensions. For in-plane problems only axial loads  $N(x,y)$  are considered. There are no lateral loads or moments. Displacement boundary conditions can be of the type  $au + bv = c$  where  $a$ ,  $b$ , and  $c$  are specified coefficients; and  $u$  and  $v$  are displacements. In plane forces may also be specified on portions of the boundary where displacement is not specified.

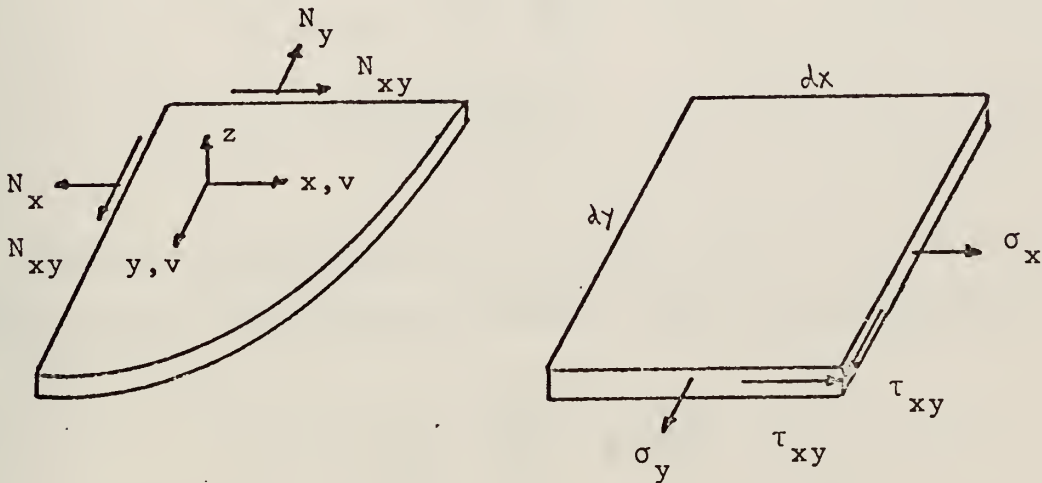


Figure A-1. The In-Plane Problem

Since  $h$  is small in comparison with the plane dimensions,  $\sigma_z \ll \sigma_x, \sigma_y$  and  $\tau_{zx}, \tau_{zy} \ll \tau_{xy}$ . This suggests the use of plane stress conditions, that is,  $\sigma_z, \tau_{zx}, \tau_{zy}$  are considered to be zero.

The basic stress strain relations become the plane stress equations.



$$\sigma_x = \frac{E}{1 - \mu^2} (\epsilon_x + \mu \epsilon_y)$$

$$\sigma_y = \frac{E}{1 - \mu^2} (\mu \epsilon_x + \epsilon_y)$$

$$\tau_{xy} = \frac{E}{1 + \mu} \epsilon_{xy} \quad (A-1)$$

The strain displacement relations are

$$\epsilon_x = \frac{\partial u}{\partial x}$$

$$\epsilon_y = \frac{\partial v}{\partial y}$$

$$\epsilon_z = -\mu \left( \frac{\partial u}{\partial x} + \frac{\partial v}{\partial y} \right)$$

$$\epsilon_{xy} = \frac{1}{2} \left( \frac{\partial u}{\partial y} + \frac{\partial v}{\partial x} \right) \quad (A-2)$$

Substituting Eqns. (A-2) in Eqns. (A-1), the partial differential equations for the-in plane problem become

$$\sigma_x = \frac{E}{1 - \mu^2} \left[ \frac{\partial u}{\partial x} + \mu \frac{\partial v}{\partial y} \right]$$

$$\sigma_y = \frac{E}{1 - \mu^2} \left[ \mu \frac{\partial u}{\partial x} + \frac{\partial v}{\partial y} \right]$$

$$\tau_{xy} = \frac{E}{2(1 + \mu)} \left[ \frac{\partial u}{\partial y} + \frac{\partial v}{\partial x} \right] \quad (A-3)$$





Stress resultants  $N_x$ ,  $N_y$ ,  $N_{xy}$  having the units of force per unit length (# in/in<sup>2</sup>) are defined as

$$N_x = \int_{-h/2}^{h/2} \sigma_x dz \quad N_{xy} = \int_{-h/2}^{h/2} \tau_{xy} dz \quad N_y = \int_{-h/2}^{h/2} \sigma_y dz$$

(A-4)

These last expressions imply internal discontinuity in stress is associated with a discontinuity in applied internal in plane-force.

For plane stress the equilibrium equations are

$$\sum F_x = 0 : \frac{\partial \sigma_x}{\partial x} + \frac{\partial \tau_{xy}}{\partial y} \rightarrow \frac{\partial N_x}{\partial x} + \frac{\partial N_{xy}}{\partial y} = 0 \quad (A-5)$$

$$\sum F_y = 0 : \frac{\partial \sigma_y}{\partial y} + \frac{\partial \tau_{xy}}{\partial x} \rightarrow \frac{\partial N_y}{\partial y} + \frac{\partial N_{xy}}{\partial x} = 0 \quad (A-6)$$

The finite element method yields a system of algebraic equations which are obtained from the above partial differential equations by the usual method as given by Zienkiewicz [Ref. 8].



## APPENDIX B

### THE FINITE ELEMENT METHOD

An extensive description of the finite element method can be found in Zienkiewicz [Ref. 8]. However to facilitate understanding of this project, certain features of the elements will be presented.

In all finite element programs certain rules must be followed in selecting the assumed displacement field.

1. The finite element displacement field must accommodate rigid body displacements.

2. At common boundaries two elements remain in continuous contact with each other. Neither gaps nor overlappings are permitted.

3. Constant straining patterns must be included in higher order descriptions of displacement.

#### CONSTANT STRAIN TRIANGLE (CST)

For the CST the  $u$  and  $v$  in-plane displacements are approximated by a linear field over each element. Since strain is the first derivative of displacement, this gives a constant strain element.



The area coordinates used in the program are defined as

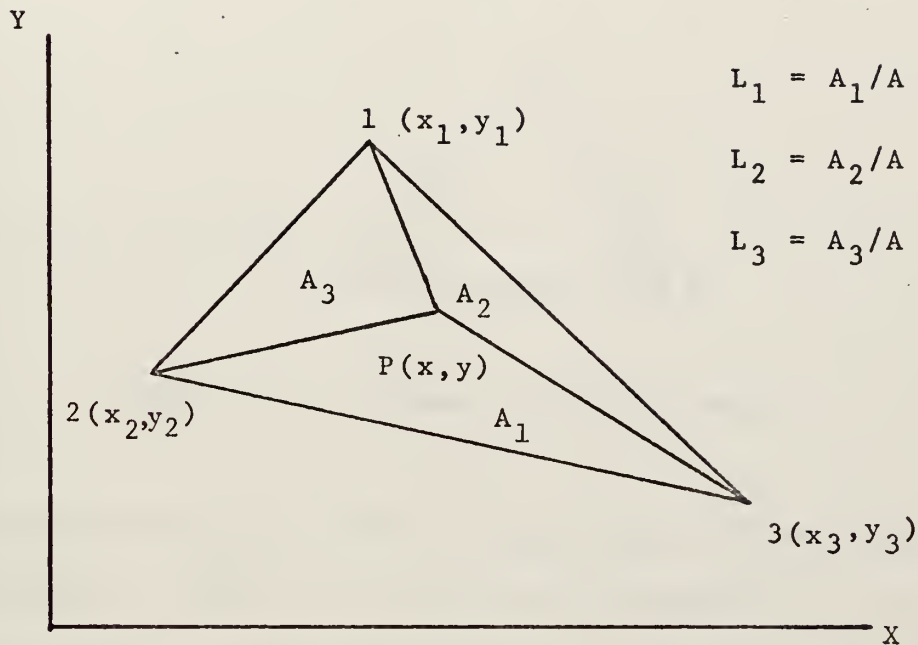


Figure B-1. Area Coordinates

With these coordinates the linear displacement field over the element is simply

$$u(x,y) = L_1 u_1 + L_2 u_2 + L_3 u_3$$

$$v(x,y) = L_1 v_1 + L_2 v_2 + L_3 v_3 \quad (B-1)$$



## LINEAR STRAIN TRIANGLE (LST)

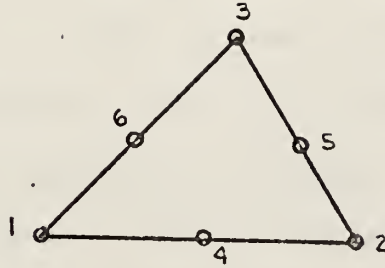


Figure B-2. Linear Strain Triangle

The LST has three nodes on each side and each displacement field is taken as a 2nd order polynomial over the element domain. The displacements  $u$  and  $v$  for each element are as follows

$$u(x,y) = N_1 u_1 + N_2 u_2 + N_3 u_3 + N_4 u_4 + N_5 u_5 + N_6 u_6 \quad (B-2)$$

$$v(x,y) = N_1 v_1 + N_2 v_2 + N_3 v_3 + N_4 v_4 + N_5 v_5 + N_6 v_6$$

where  $N_1 = 2L_1 - 1$  for a typical corner node  
 $N_4 = 4L_1 L_2$  for a typical mid side node

The  $N_i$  are called interpolation functions for the assumed displacement field. Differentiating the displacement fields gives linear strain over each element, hence the name linear strain triangle (LST).





## PLISOP

The PLISOP program was coded by Professor Gilles Cantin and his students at the Naval Postgraduate School, Monterey. It performs a plane stress or a plane strain analysis by the finite element method using numerically integrated isoparametric elements. These elements have four sides, each of which may be either curved or straight. The same shape functions which define the geometry also are used to describe the displacement. The strains will be a function of the number of nodes per side of the element. The comparisons made in this thesis were to a cubic element. This isoparametric element uses a cubic displacement field and yields parabolic strain (stress) fields over each element.

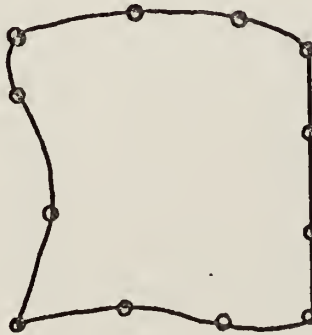


Figure B-3. 12 Node PLISOP Element

All of these elements, the CST, LST and PLISOP, with displacements being the only degrees of freedom, yield discontinuous stresses along element interfaces. The CBM gives continuous stress along element boundaries.



For each of the conventional finite elements, the order of the strain approximation is one less than the order of the displacement approximation. However for the CBM the displacement approximation and the strain approximation are of the same order.



# APPENDIX C COMPUTER PROGRAM

```

COMMON/PLACE/GRANK(242,34),P(242),W(242)
COMMON/STOCK/X(2,200),T(200),C(3,3),PV(242),
1U(3,6),ZK(6,6),CF(3,3),UBC(36),
2CM(3,3),A1(200),A2(200),A3(200),B1(200),B2(200),B3(200),A(200),
3STRN1(200),STRN2(200),TAU1(200),TAU22(200),STRN12(200),
4TAU12(200),TAJ44(200),ITEM(200,3),NUDISP(24),NNX(10),NNY(10)
5NOLJ(10),NBOY(68),ITEM(200,3),GFM(121,121)
DIMENSION EFM(3,3),GFM(121,121)
DIMENSION GRAN(242,34)
REAL*8 TITLE(10)
DATA TITLE/, GFM, ',' MATRIX ',8*0.0/
DIMENSION IPROB(10)

      READ(5,3) LOOP
      WRITE(6,3) LOOP
      3 FORMAT('1',2X,'THIS IS LOOP NUMBER',I5)

```

\*\*\*\*\*

```

DO 600J LOP=1, LOOP

```

```

      NUMEL = NUMBER OF ELEMENTS
      NUMNP = NUMBER OF NODAL POINTS
      NBAN = HALF BAND WIDTH OF STIFFNESS MATRIX
      NUMDF = NUMBER OF DEGREES OF FREEDOM, DOF
      NMATF = NUMBER OF ELEMENTS IN THE FILAMENT
      NFNP = NUMBER OF NODES IN THE FILAMENT
      INMNP = INITIAL MATRIX NODAL POINT X BOUNDRY
      NELBX = NUMBER OF ELEMENTS ON THE X BOUNDRY
      NPROB = NUMBER OF PROBLEMS

```

```

      READ(5,80) NUMEL,NUMNP,NBAN,NUMDF,NMATF
      WRITE(6,81) NJMEL,NBAN,NUMNP,NBAN,NUMDF,NMATF
81 1',I5,2X,'NMATF =',I5)

```

```

      READ(5,80) NFNP,INMNP,NELBX,NELBY,NPROB
      WRITE(6,82) NFNP,INMNP,NPROB
82 FORMAT(2X,'NFNP =',I5,2X,'INMNP =',I5,2X,'NPROB =',I5)
      READ(5,60) (IPROB(I),I=1,NPROB)
      WRITE(6,85) (I,IPROB(I),I=1,NPROB)

```

```

      READ(5,20) ((X(I,J),I=1,2),J=1,NUMNP)
      WRITE(6,25) (J,X(1,J),X(2,J),J=1,NUMNP)

```

```

      READ(5,30) ((ITEM(I,J),J=1,3),T(I),I=1,NUMEL)
      WRITE(6,35) (I,T(I),(ITEM(I,J),J=1,3),I=1,NUMEL)

```



```

C
41 READ(5,40) ((CF(I,J),J=1,3),I=1,3)
   READ(5,40) ((CM(I,J),J=1,3),I=1,3)
   WRITE(6,41)
   FORMAT(/,2X,'FILAMENT CONSTITUTIVE RELATION MATRIX',-//)
   WRITE(6,45) ((CF(I,J),J=1,3),I=1,3)
   WRITE(6,42)
42 FORMAT(/,2X,'MATRIX CONSTITUTIVE MATRIX',-//)
   WRITE(6,45) ((CM(I,J),J=1,3),I=1,3)
   READ(5,20) POISF,POISM
   WRITE(6,50) EF,EM
   WRITE(6,21) POISF,POISM
21 FORMAT(2X,'POISSON RATIO FOR THE FILAMENT IS',F10.5,'AND FOR THE
   1 MATRIX IS',F10.5)
55 WRITE(6,55) EF,EM
   FORMAT(2X,'YOUNGS MODULUS FOR THE FILAMENT IS',F10.0,'AND FOR THE
   1 MATRIX IS',F10.0)
C
C
   READ(5,90) AVETHK
   WRITE(6,95) AVETHK
C
C *****
C FORMAT STATEMENTS
C *****
C 10 FORMAT(8I10)
C
C 15 FORMAT(2X,'NUMBER OF ELEMENTS =',I5//2X,'NUMBER OF NODAL POINTS =',
   1,I5//2X,'MAXIMUM WIDTH OF MATRIX GRANK=',I5//2X,'NUMBER OF DEGR
   2 EES OF FREEDOM=',I5//2X,'NUMBER OF APPLIED LOADS =',I5//2X,'NUMBER
   3 OF BOUNDARY CONDITIONS =',I5//2X,'NUMBER OF NON ZERO DISPLACE
   4 MENT BC=',I5//2X,'NUMBER OF FILAMENT ELEMENTS=',I5)
C
C 20 FORMAT(2F10.5)
C
C 25 FORMAT(5X,'SYSTEM NODAL POINT NO. =',I5,5X,'X(1) COORD. =',F10.5,
   15X,'X(2) COORD. =',F10.5)
C
C 30 FORMAT (3I10,F10.5)
C
C 35 FORMAT(2X,'ELEMENT NO.',I5,2X,'HAS THICKNESS=',F10.5,2X,'NODE(1)
   1 IS AT',I5,2X,'NODE(2) IS AT',I5,2X,'NODE(3) IS AT',I5)
C
C THE C(I,J) ARE THE COEFFICIENTS IN THE STRESS-STRAIN MATRIX
C
C 40 FORMAT (3F10.5)
C 45 FORMAT (1H3/(1X,3E20.8))
C 50 FORMAT(2F10.3)

```













```

      NG=ITEM(IX,K)
      GFM(ND,NG)=GFM(ND,NG)+EFM(J,K)
222 CONTINUE
224 CALL GETIME(IT)
      TIME=IT*.000026*92
      IF(ISK.EQ.0) WRITE(6,225) TIME
225 FORMAT(5X,'TIME TO ASSEMBLE GFM IS',1G15.4,'SECONDS')
      ISK=1
      U(1,1)=B1(IX)/(2.*A(IX))
      U(1,2)=0.
      U(1,3)=B2(IX)/(2.*A(IX))
      U(1,4)=0.
      U(1,5)=B3(IX)/(2.*A(IX))
      U(1,6)=0.
      U(2,1)=0.
      U(2,2)=A1(IX)/(2.*A(IX))
      U(2,3)=0.
      U(2,4)=A2(IX)/(2.*A(IX))
      U(2,5)=0.
      U(2,6)=A3(IX)/(2.*A(IX))
      U(3,1)=A1(IX)/(2.*A(IX))
      U(3,2)=B1(IX)/(2.*A(IX))
      U(3,3)=A2(IX)/(2.*A(IX))
      U(3,4)=B2(IX)/(2.*A(IX))
      U(3,5)=A3(IX)/(2.*A(IX))
      U(3,6)=B3(IX)/(2.*A(IX))
      DO 310 I=1,6
      DO 310 J=1,6
      ZK(I,J)=0.
      DO 300 K=1,3
      DO 300 L=1,3
      ZK(I,J)=ZK(I,J)+U(K,I)*C(K,L)*U(I,J)
300 CONTINUE
310 CONTINUE
      DO 320 I=1,6
      DO 320 J=1,6
      ZK(I,J)=A(IX)*T(IX)*ZK(I,J)
320 CONTINUE
      C
      C
      C ASSEMBLY OF THE SYSTEM STIFFNESS MATRIX, DENOTED GRANK
      C
      C
      C
      DO 995 J=1,3
      II=2*(ITEM(IX,J)-1)
      DO 990 K=1,3

```



```

III=2*(ITEM(IX,K)-1)
IF(III.GT.III) GO TO 990
III=III-III
DO 900 L=1,2
JJ=III+L
LL=2*(J-1)+L
M=1
IF(III.EQ.0) M=L
DO 900 N=M,2
MM=2*(K-1)+N
KK=III+N-L+1
IF(KK.GT.NBAN) NBAN=KK
GRANK(JJ,KK)=GRANK(JJ,KK)+ZK(LL,MM)
GRAN(JJ,KK)=GRANK(JJ,KK)
CONTINUE
900 CONTINUE
990 CONTINUE
995 CONTINUE
1000 CONTINUE
CALL SYINV(GFM,121)
↓
C
C DO PROBLEMS I,II AND III
C
C DO 5000 NPR=1,NPROB
C MPROB=IPROB(NPR)
C
C 1 READ(5,10) NUMEL,NUMNP,NBAN,NUMDF,NAL,NBC,NUBC,NMATF
C WRITE(6,15) NUMEL,NUMNP,NBAN,NUMDF,NAL,NBC,NUBC,NMATF
C
C IF(NAL.EQ.0) GO TO 5
C READ(5,51) (NLO(I),PV(I),I=1,NAL)
C WRITE(6,56) (I,NLO(I),PV(I),I=1,NAL)
C
C 5 READ(5,60) (NBDY(I),I=1,NBC)
C WRITE(6,65) (I,NBDY(I),I=1,NBC)
C IF(NUBC.EQ.0) GO TO 1010
C READ(5,70) (NUDISP(I),UBC(I),I=1,NUBC)
C WRITE(6,75) (NUDISP(I),UBC(I),I=1,NUBC)
C
C 1010 CONTINUE
C IF(MPROB.NE.3) GO TO 1020
C READ(5,62) UNIFEZ
C WRITE(6,63) UNIFEZ
C 1020 CONTINUE
C IF(MPROB.NE.7) GO TO 1030
C READ(5,62) UNIFEZ
C WRITE(6,63) UNIFEZ
C 1030 CONTINUE

```





```

C *****
C INPUT THE APPLIED LOAD VECTOR
C *****
DO 1100 I=1,NJMDF
1100 P(I)=0.
      IF(NAL.EQ.0) GO TO 1160
      DO 1150 I=1,NAL
      JJ=NULO(I)
      P(JJ)=PV(I)
1150 *****
C *****
C REVERSE GRANK TO ACCOMODATE BOUNDARY CONDITIONS
C *****
1160 DO 1190 I=1,NBC
      JJ=NBDY(I)
      DO 1180 J=2,NBAN
      KK=JJ-J+1
      GRANK(JJ,J)=0.
      IF (KK.LT.1) GO TO 1180
      GRANK(KK,J)=0.
      CONTINUE
1180 GRANK(JJ,1)=1.
      P(JJ)=0.
1190 CONTINUE
C *****
C REVERSE GRANK TO ACCOMODATE NON ZERO DISPLACEMENT B.C.'S
C *****
      IF(NUBC.EQ.0) GO TO 1405
      DO 1400 I=1,NUBC
      JJ=NUJISP(I)
      JJJ=JJ-NBAN+1
      IF(JJJ.GT.1) GO TO 1300
      JJJ=1
      FORMAT(2I10,F10.5)
      DO 1350 J=JJJ,JJ
      K=JJ-J+1
      P(J)=P(J)-GRANK(J,K)*UBC(I)
      CONTINUE
      KK=JJ+1
      KKK=JJ+NBAN-1
      IF(KKK.LT.NUMDF) GO TO 1355
      KKK=NJMDF
      DO 1360 J=KK,KKK
      JJJ=J-JJ+1
      P(J)=P(J)-GRANK(JJ,JJJ)*UBC(I)
      CONTINUE
1455
1300
1350
1355
1360

```



```

C
DO 1380 M=1,NBAN
KK=JJ-M+1
GRANK(JJ,M)=0.
IF(KK.LT.1) GO TO 1380
GRANK(KK,M)=0.
CONTINUE
1380
C
GRANK(JJ,1)=1.
P(JJ)=UBC(I)
CONTINUE
1400
C *****
C SOLUTION OF THE DISPLACEMENT-FORCE EQUATION FOR DISPLACEMENT
1450 FORMAT(2X,'THE FORCE AT DOF',I5,'IS',F20.8) *****
C *****
C 1405 CALL BANDEC(GRANK,P,NUMDF,NBAN,1,242,34,1)
C *****
C PRINT OUTPUT *****
C *****
WRITE(6,1990)
1990 FORMAT(1,'5X','THE DISPLACEMENT SOLUTION')
2000 WRITE(6,2000) (I,P(I),I=1,NUMDF)
2000 FORMAT(2X,'DEGREE OF FREEDOM',I5,'IS DISPLACED',F20.8)
DO 1410 I=1,NUMDF
W(I)=P(I)
P(I)=0.
CONTINUE
1410
CCCC
CCCC
CCCC
CCCC
CALCULATE LOADS AT NODAL POINTS F=K*U
CALL MULI(NUMDF,NBAN,P,GRAN,W)
WRITE(6,1449)
1449 FORMAT(1,'5X','THE NODAL LOADS')
WRITE(6,1450) (I,P(I),I=1,NUMDF)
CCCC
CCCC
CCCC
CCCC
CALCULATE STRESSES AT THE NODAL POINTS
SUMFZ=0.
CCCC

```







```

TAU22(IX)=C(1,2)*STRN11(IX)+C(1,1)*STRN22(IX)
TAU12(IX)=C(3,3)*STRN12(IX)
TAU44(IX)=POIS*(TAU11(IX)+TAU22(IX))
ZFORCE=TAU44(IX)*A(IX)
C 1600 CONTINUE
C
C
C 1571 WRITE(6,1571)
      FORMAT(1,20X,'CENTROIDAL STRESSES',//)
C 1573 WRITE(6,1573)
      FORMAT(16X,'ELEMENT',8X,'TAU11',15X,'TAU22',15X,'TAU12',15X,'TAU44')
      1,
      WRITE(6,1572) (IX,TAU11(IX),TAU22(IX),TAU12(IX),TAU44(IX),IX=1,
      1 NUMEL)
C 1572 FORMAT(10X,I10,4E20.8)
C *****
C C USE CONJUGATE BASIS METHOD TO CALCULATE NODAL STRESSES
C *****
C 4799 WRITE(6,4799)
      FORMAT(1,20X,'NODAL STRESSES USING CONJUGATE BASIS METHOD',//)
C 4650 WRITE(6,4650)
      FORMAT(16X,' NODE ',7X,'GTAU11',14X,'GTAU22',14X,'GTAU12',14X,
      1,'GTAU44')
      CALL SETIME
      DO4800 I=1,NUMNP
      GTAU11=0.0
      GTAU22=0.0
      GTAU12=0.0
      GTAU44=0.0
      DO4600 J=1,NUMEL
      DO4400 N=1,3
      IHC=ITEM(J,N)
      GTAU11=GTAU11+(A(J)/3.)*TAU11(J)*GFM(IHC,I)
      GTAU22=GTAU22+(A(J)/3.)*TAU22(J)*GFM(IHC,I)
      GTAU12=GTAU12+(A(J)/3.)*TAU12(J)*GFM(IHC,I)
      GTAU44=GTAU44+(A(J)/3.)*TAU44(J)*GFM(IHC,I)
      CONTINUE
C 4400 CONTINUE
C 4600 WRITE(6,4700)(I,GTAU11,GTAU22,GTAU12,GTAU44)
C 4700 FORMAT(10X,I10,4E20.8)
C 4800 CONTINUE
      CALL GETIME(IL)
      TIME=IL*.000026
      WRITE(6,4801) TIME

```





```

4801 FORMAT(5X,'TIME TO GET NODAL STRESS IS',F15.4,'SECONDS')
5000 CONTINUE
C
C 6000 CONTINUE
C      STOP
C      END

```

↑



96







```

C
C
C
C
SUBROUTINE MULI (NUMDF, NBAN, F, S, U)
  DIMENSION F(242), S(242, 34), U(242)
  SUBROUTINE MULI FULL MULTIPLIES A SYMMETRIC BANDED MATRIX WITH A VECTOR

  DO 120 J=1, NUMDF
    M=MINO(NBAN, NUMDF+1-J)
    DO 105 K=1, M
      L=J+K-1
      F(J)=F(J)+S(J, K)*U(L)
    CONTINUE
    IF(J.EQ.1) GO TO 120
    L=MINO(J-1, NBAN-1)+1
    DO 110 K=2, L
      M=J-K+1
      F(J)=F(J)+S(M, K)*U(M)
    CONTINUE
  CONTINUE
120 RETURN
C
C
END

```





## LIST OF REFERENCES

1. Oden, J. T., and Brauchli, H. J. "On the Calculation of Consistent Stress Distribution in Finite Element Approximations," International Journal for Numerical Methods in Engineering, v. 3, p. 317-325, 1971.
2. Oden, J. T., Finite Elements of Nonlinear Continua, McGraw-Hill, 1972.
3. Wilson, E. L., Finite Element Analysis of Two-Dimensional Structures, Ph.D. Thesis, University of California, Berkeley, 1963.
4. Turner, M. J., Martin, H. L., Weikel, B. C., "Further Developments and Applications of the Stiffness Method," Matrix Methods Structural Analysis, Agard 72, 203-266 (1964).
5. Gallagher, R. H., A Correlation Study of Methods of Matrix Structural Analysis, Pergamon Press, 1964.
6. Lin, T. H., Salinas, D. and Ito, Y. M., "Initial Yield Surface of an Undirectionally Reinforced Composite," Journal of Applied Mechanics, Paper No. 71-APMN-21.
7. Felippa, C. A., Refined Finite Element Analysis of Linear and Nonlinear Two Dimensional Structures, University of California, Berkeley, Department of Civil Engineering, Report 66-22.
8. Zienkiewicz, O. C., The Finite Element Method in Engineering Science, McGraw-Hill, 1971.



# INITIAL DISTRIBUTION LIST

No. Copies

1. Defense Documentation Center 2  
Cameron Station  
Alexandria, Virginia 22314
2. Library, Code 0212 2  
Naval Postgraduate School  
Monterey, California 93940
3. Asst. Professor D. Salinas, Code 59Zc 1  
Department of Mechanical Engineering  
Naval Postgraduate School  
Monterey, California 93940
4. Professor G. Cantin, Code 59Ci 1  
Department of Mechanical Engineering  
Naval Postgraduate School  
Monterey, California 93940
5. Department of Mechanical Engineering 1  
Naval Postgraduate School  
Monterey, California 93940
6. Lieutenant W. H. Conley, Jr. USN 1  
Naval Safety Center  
NAS, Norfolk, Virginia 23511



## DOCUMENT CONTROL DATA - R &amp; D

(Security classification of title, body of abstract and indexing annotation must be entered when the overall report is classified)

ORIGINATING ACTIVITY (Corporate author)

Naval Postgraduate School  
Monterey, California 93940

2a. REPORT SECURITY CLASSIFICATION

Unclassified

2b. GROUP

REPORT TITLE

Consistent Stresses for the  
Finite Element Stiffness Method

DESCRIPTIVE NOTES (Type of report and, inclusive dates)

Master's Thesis; December 1972

AUTHOR(S) (First name, middle initial, last name)

William H. Conley, Jr.

REPORT DATE

December 1972

7a. TOTAL NO. OF PAGES

102

7b. NO. OF REFS

8

8. CONTRACT OR GRANT NO.

9a. ORIGINATOR'S REPORT NUMBER(S)

b. PROJECT NO.

9b. OTHER REPORT NO(S) (Any other numbers that may be assigned  
this report)

10. DISTRIBUTION STATEMENT

Approved for public release; distribution unlimited.

11. SUPPLEMENTARY NOTES

12. SPONSORING MILITARY ACTIVITY

Naval Postgraduate School  
Monterey, California 93940

13. ABSTRACT

Conjugate basis functions which are continuous throughout a model are used to approximate a stress field. This conjugate approximation has less mean error than approximations calculated using conventional finite element methods and is a better approximation at extreme values of stress. This thesis consists of two major parts. The appropriate analytic expressions for conjugate stress fields are set forth and applied to the constant strain triangle finite element. Analyses are then performed with these new stress calculations and the results compared to some previous stress calculations.



4. KEY WORDS	LINK A		LINK B		LINK C	
	ROLE	WT	ROLE	WT	ROLE	WT
Conjugate Basis  Finite Element						









Thesis  
C7025  
c.1

Conley

Consistent stresses  
for the finite element  
stiffness method.

141267

thesC7025

Consistent stresses for the finite eleme



3 2768 002 09318 9

DUDLEY KNOX LIBRARY